Proteomic and Lipidomic Analyses of Lipid Body Isolated from the Alkenone-producing Marine Haptophyte Alga *Tisochrysis lutea*

A Dissertation submitted to

the Graduate School of Life and Environmental Sciences,

the University of Tsukuba

in Partial Fulfillment of the Requirements

for the Degree of Doctor of Philosophy in Science

(Doctoral Program in Biological Sciences)

SHI QING

Table of content

Abbreviations

AB, alkenone body;

CCMP, culture collection of marine phytoplankton at National Center for Marine Algae and Microbiota (NCMA) of Bigelow Laboratory);

cDNA, complementary DNA;

CoA, coenzyme A;

DNA, deoxyribonucleic acid;

DW, deionized water;

emPAI, exponentially modified Protein Abundance Index

ER, endoplasmic reticulum;

EST, expressed sequence tag;

ESM, Erd-Schreiber's medium;

GC-FID, gas chromatography equipped with flame ionization detector;

GC-MS, gas chromatography equipped with mass spectrometry;

LB, lipid body;

LB-TT, lysis buffer containing thiourea and tris(hydroxymethyl)aminomethane (Tris);

LC-MS/MS. liquid chromatography coupled with tandem mass spectrometry

MA, Marine Art SF(artificial seawater);

NCBI, National Center for Biotechnology Information;

OD_{750}, optical density at 750nm

PNS, post-nuclear supernatant;

RNA, ribonucleic acid;

RuBisCO, ribulose-1,5-bisphosphate carboxylase/oxygenase;

SDS-PAGE, sodium dodecyl sulfate polyacrylamide gel electrophoresis;

Abstract

Due to the increasing interest in biofuels such as biodiesel, many researches have focused on plant lipid/oil production. The production of lipids/oils in plants is driven by photosynthesis including fixing atmospheric CO_2 and associated carbon metabolism. When lipids, products of photosynthesis, is changed to biodiesels via chemical processes and used for producing energy and biomass products, CO_2 is just emitted to the atmosphere as a waste. Therefore, plant lipids are said as "renewable energy". However, biofuel production by land plants, especially crops, was reported to require huge land and induce economical problems. Instead, oil-producing microalgae have recently gathered keen interests since the efficiency of lipid/oil production by microalgae was reported to be very high in comparison with land plants.

Microalgae produce lipids/oils and the products are triacylglycerol (TAG) as neutral lipid for storage and various fatty acids as membrane components. However, there are some unique microalgae which produce hydrocarbon molecules as storage lipids/oils. There are several hydrocarbons which can be used directly as biofuel, as known as a drop-in-fuel. In this study, I focused on the lipid metabolism in marine microalgae which are known as long-chain ketones and alkenes producers expected to be useful biofuels.

As a research material, I selected the marine phytoplankton *Tisochrysis lutea* which is classified as the haptophyte alga and known as the secondary symbiotic organism. This alga produces special types of lipid molecules as long-chain ketones, named alkenones, instead of universal reserve glycerolipids such as TAG. So far, only five species in a group of haptophytes are known to produce alkenones. Alkenones are unique in their length (C_{37}-C_{40}), having two to four *trans*-double bonds and one *keto*-group in a molecule, which is commonly thought to be the molecular source of petroleum produced mainly in the Cretaceous era. Alkenones are also widely used as biomarkers for the reconstruction of paleotemperature of ancient ocean surface since the number of double bonds in a molecule shows a strong dependence on temperature during growth of the organisms. However, the cellular machinery for their production largely remains unknown.

In the previous study in the laboratory, alkenones were suggested to be stored in membrane compartments. In higher plants, lipid bodies composed of lipids such as TAG, fatty acids and some proteins that are associated with lipid metabolism. In plant seeds, oleosins are found to

be the major protein which plays an important function for the formation and stabilization of lipid bodies. Although lipid bodies with TAG were already well characterized, only few examples were reported in TAG-producing microalgae. However, almost no information is available in the microalgae that produce lipids/oils without TAG, such as alkenones and alkenes. How such alkenones and alkenes are produced metabolically? In order to elucidate the mechanism, I studied the mechanism of lipid body production in an alkenone-producing haptophyte *T. lutea*.

Lipid body (LB) is recognized as the cellular carbon and energy storage organelle in many organisms. Similarly, LBs have been observed in the marine haptophyte alga *T. lutea* which produces special lipids such as alkenones, but not TAG. My study in this thesis is composed of three parts: i) establishment of a protocol for the isolation and purification of LBs from *T. lutea*, ii) analysis of lipid composition in the purified LBs, and iii) proteomic analysis of the purified lipid bodies.

Firstly, I established a method for LB isolation from the haptophyte *T. lutea* by modifying previously reported methods. Two important points were especially needed to be developed for the successful isolation and purification of LBs of *T. lutea* in this study. The first point was related to the preparation of very large LB-harboring cells that are obtained by growing/maintaining cells under nitrogen-deficient conditions for two weeks. N-deficient culture was also effective to decrease the amount of ribulose-1,5-bisphosphate carboxylase/oxygenase (Rubisco) which generally disturbs purification quality as a contaminant in LB fraction. Degradation of chloroplasts was experimentally confirmed by the absence of chlorophyll auto-fluorescence under a fluorescent microscope. The second point was the utilization of six different sucrose density layers in a sucrose density gradient centrifugation to result in the enhancement of cleaning effect of LBs by washing and removing all visible debris and membranes derived from broken cells. Purity of isolated LBs was confirmed by the absence of chlorophyll auto-fluorescence and no contamination of the most abundant cellular protein, Rubisco, using an anti-Rubisco antibody. According to the method developed, I was able to obtain highly purified lipid body preparation isolated from the haptophyte alga *T. lutea* for the first time according to literatures.

Secondly, components of the purified LBs of *T. lutea* were analyzed by a gas

chromatography with a Flame Ionization Detector (GC-FID). Then, I found that the LBs contain C_{37} and C_{38} alkenones as major components and alkenes as minor components and therefore the LB can more appropriately be named as "alkenone body (AB)".

Thirdly, proteomic analysis was performed. For the process, proteins extracted from the ABs were analyzed by the combination of 1DE (SDS-PAGE) and tandem mass spectrometry for confident protein identification and annotated using BLAST tools at NCBI. Totally 514 proteins were identified at the maximum. The homology search identified three major proteins, V-type H^+-ATPase (V-ATPase), a hypothetical protein EMIHUDRAFT_465517 found previously in other alkenone-producing haptophytes, and a lipid raft–associated SPFH domain-containing protein. The data suggest that ABs of *T. lutera* are surrounded by a lipid membrane originating from either the endoplasmic reticulum (ER) or the ER derived from chloroplast outermost envelopes and function as the storage organelle of alkenones.

The present study in the alkenone-producing haptophyte *T. lutea* fulfilled the three main objectives, namely the establishment of a method of AB-isolation, clear metabolomic evidence on the presence of AB and proteome dataset proposing a unique structure of ABs. Finally, this study revealed the presence of V-ATPase as a major protein in ABs of *T. lutea*, and then that the ABs might be derived from the ER. Furthermore, I speculate that the abundant hypothetical protein EMIHUDRAFT_465517 might be strongly related with alkenone metabolism since that protein showed high similarity with alkenone-producers. These are first findings on lipid body structure in non-TAG but alkenone/alkene-producing microalgae.

1 Introduction

1.1 Haptophyte algae

Marine haptophyte algae are known to be globally distributed as one of the greatest producers of biomass in the oceans (Liu et al., 2009). Haptophytes comprise both calcifying species, called coccolithophores, and non-calcifying species. *Emiliania huxleyi* (Isochrysidales) is one of the cosmopolitan species of coccolithophores and known to produce huge blooms that are often observed from satellite such as SeaWiFs especially at high latitude oceans (Holligan et al., 1983). Therefore, *E. huxleyi* is regarded as an important player in transporting atmospheric CO_2 to the ocean sediment as calcium carbonate and organic matter by functioning as the biological pump.

On the other hand, a non-calcareous marine haptophyte species *Tisochrysis lutea*, previously named as *Isochrysis* aff. *galbana* (Clone Tahiti) as a taxonomic variation of *Isochrysis* species (Bendif et al., 2013), not known as bloom-producing alga in the ocean has been well-studied in aquaculture research for its mass cultivation as a commercial feed for fish (Marchetti et al., 2012; Alkhamis and Qin, 2013). In particular, lipids of *T. lutea* are broadly used as a suitable nutrition source for the larvae due to the presence of high amounts of long-chain polyunsaturated fatty acids such as docosahexaenoic acid (DHA) in their contents (Brown et al., 1993; Liu and Lin, 2001). *T. lutea* is clearly genetically distinct from *Isochrysis galbana (Not et al., 2012)*, and biochemically, there are also some differences like their lipid content in sterol (Dorrell and Smith, 2011) and DHA (Liu and Lin, 2001). And *T. lutea* can be grown very fast over a temperatures range which is much broader than *I. galbana* (Holligan et al., 1983).

Interestingly, most of the species in Isochrysidales also produce unique neutral lipid molecules of long-chain ketones, called alkenones (Marlowe et al., 1984; Marlowe et al., 1984; Sukenik and Wahnon, 1991), instead of the universally stored glycerolipids such as triacylglycerol (TAG). Alkenones have been identified as the major neutral lipids in *T. lutea* (Marlowe et al., 1984). Alkenones are also typical in their carbon chain length (from C_{37} to C_{40}) and carry two to four *trans*-type double bonds and one *keto*-group (Rechka and Maxwell, 1988). So far, only five strains of haptophytes in the order Isochrysidales are known to produce alkenones (Marlowe et al., 1984; Theroux et al.,

2010). The number of unsaturated bonds in a molecule of alkenone is known to increase when cells are grown or maintained at low temperature. Because of this, alkenones have been widely used as biomarkers for the reconstruction of marine paleo-temperature in geological studies by determining the unsaturation index, $U^{K'}_{37}$, calculated as a parameter of the ratio of $C_{37:2}$ to $C_{37:3}$ alkenones (Prahl and Wakeham, 1987; Prahl et al., 2000). Previous studies have suggested that alkenones are stored in organelles known as lipid bodies (LBs) and function as a storage lipid in the cells (Liu and Lin, 2001; Eltgroth et al., 2005). According to geological survey, alkenones are generally regarded as one of the sources for petroleum generated in geological history such as in the Cretaceous period (Sukenik and Wahnon, 1991; Rodolfi et al., 2009; O'Neil et al., 2014). As such, alkenones have garnered broad interests in geological, biological and industrial fields, but the cellular machinery and metabolic process for their production remained largely unknown (Bell and Pond, 1996; Epstein et al., 2001; Sawada and Shiraiwa, 2004).

1.2 Lipid body associated proteins

LBs widely existing in eukaryotic cells are generally believed to be the storage center of TAG (Farese and Walther, 2009; Krahmer et al., 2009). Recent studies of TAG-producing LBs (Fig. 1), however, have revealed that LBs might also serve as a storage organelle for endogenous proteins, and that these proteins carry diverse functions in lipid metabolism, cell signaling, intracellular trafficking, and protection against pathogen infection (Cermelli et al., 2006; Goodman, 2008; Murphy et al., 2009; Zehmer et al., 2009; Chapman et al., 2012; Li et al., 2012; Zechner et al., 2012; Shimada et al., 2014). It is generally accepted that oleosins and caleosins function as structural proteins in LBs of higher plants while steroleosins appear to have played a role in signal transduction (Naested et al., 2000; Lin et al., 2002; Siloto et al., 2006). Also, in seed oil bodies of *Arabidopsis thaliana*, a member of the short-chain steroid dehydrogenase reductase superfamily, was identified although its function is not properly known yet (d'Andrea et al., 2007).

In the green alga *Chlamydomonas reinhardtii*, the major lipid droplet protein

(MLDP) was shown to be a structural protein of LBs (Moellering and Benning, 2010; Nguyen et al., 2011). MLDP was also found in the salt-tolerant green alga *Dunaliella* sp. (Davidi et al., 2012). Others examples are a Haematococcus oil globule protein (HOGP) in *Haematococcus pluvialis* (Peled et al., 2011), a primitive caleosin in *Chlorella* sp. (Lin et al., 2012), and a lipid droplet surface protein (LDSP) in *Nannochloropsis* sp. (Vieler et al., 2012) and SLDP in *Symbiodinium* spp. (Pasaribu et al., 2014).

It is commonly assumed that LBs in higher plants are likely to be formed by budding from the ER (Heldt and Piechulla, 2011); while in microalgae such as *C. reinhardtii* (Goodson et al., 2011) and *T. lutea* the location where LBs arise from is still a mystery. Glycerol-3-phosphate acyltransferase MmGPAT3, lysophosphatidic acid acyltransferase (LPAT1) and phospholipid:diacylglycerol acyltransferase (PDAT) were detected in LBs of *C. reinhardtii* (Nguyen et al., 2011) and therefore are very likely related to oil biosynthesis. This kind of information can help to interpret lipid metabolism in LBs. However, LBs in alkenone-producing, but no or very low amounts of TAG, organisms as well as the secondary symbiotic organisms have not yet been properly characterized. Moreover, the mechanism of LB formation including site information is virtually unknown. Revealing the proteins associated with LBs in the marine haptophyte *T. lutea* can provide new insights on where and how these alkenone-dominant LBs are formed in addition to understanding alkenone metabolism. Furthermore, a better understanding of the LB proteome will certainly aid in exploring the unique features of LBs and the lipid production mechanism in non-TAG-producing organisms.

1.3 Aims of this study

In other algea, the major lipid content of body is TAG and TAG synthesis mainly occurs by following the glycerol phosphate pathway. Most of the enzymes participated in TAG synthesis exist on ER or mitochondria (Metzger and Largeau, 2005), and after budding from ER how the lipids were transferred to lipid bodies were still unknow. In *T. lutea*, the secondary symbiotic organism, currently there is no information on the

synthetic pathway of alkenone producing, whether this neutral lipids are following similar pathway in other microalgae is a myth. Besides, it is long been a puzzle whether the alkenone is really located in lipid bodies of *T. lutea* is completely unknown due to the limitation of lipid bodies isolation technic.

Therefore, in the present study, my focus is three-fold: i) establishment of a protocol for the isolation and purification of LBs from the haptophyte *T. lutea*, ii) analysis of the lipid composition in the purified LBs, and iii) proteomic analysis of the purified LBs.

Briefly, the LBs were isolated and purified by a newly developed method that utilized a sucrose density gradient centrifugation with stepwise sucrose density layers, followed by their purity check and proteomic analysis using 1DE (SDS-PAGE) linked to tandem mass spectrometry to reveal the LB proteins. To my knowledge, this report is the first inventory of *T. lutea* LB proteome, which could serve as a valuable resource for researchers studying alkenone producing algae including lipid metabolism and biofuel production since alkenones are one of important candidates for the production of algal biofuels (Bougaran et al., 2012).

2 Materials and study methods

2.1 Organism and culture conditions

The haptophyte alga *Isochrysis* aff. *galbana* (Clone Tahiti) (also referred to as T-Iso) examined in this study, which was recently renamed as *Tisochrysis lutea* (Bendif et al., 2013), was obtained from the Matsunaga laboratory, Tokyo University of Agriculture and Technology. This strain has been maintained in our laboratory for about 15 years.

During this study, the cells were grown in a 20-L polycarbonate carboy (Nalgene) containing artificial seawater, Marine Art SF-1 (Tomita Seiyaku Co., Ltd., Tokyo, Japan) enriched with the Erd–Schreiber's medium (MA-ESM), and soil extracts that were replaced by 10 nM sodium selenite (Danbara and Shiraiwa, 1999). The MA-ESM also contains 1.4 mM sodium nitrate (120 mg/L). Salinity of the medium was modulated to 30‰ using a Refractometer (MASTER-S/MillM, ATAGO Co. Ltd., Tokyo, Japan) before adding ESM and sodium selenite.

Cells used for the experiments were grown at 20 ℃ for 2 weeks until they reached stationary growth phase. I used RQflex Plus Reflectometer (Merck, Darmstadt, Germany) with Reflectoquant (Test Strip) for nitrate test (Merck) in a separate experiment under same condition (unpublished data).

For nitrogen-deficient culture, cells were transferred to nitrogen-depleted medium lacking sodium nitrate (−N medium) after washing once with −N medium by centrifugation (5 min at 4,000 ×*g*). Cells were separated into 6 oblong glass vessels after re-suspension into −N medium and then grown under constant illumination (100 μmol photons m^{-2} s^{-1}) and aeration (100 mL/min) at 20 ℃ for about 2 weeks.

2.2 Lipid body isolation

The protocol for isolation of LB was established with reference to a previous study (Ding et al., 2013) with modifications. I briefly describe this modified protocol as follows.

The algal cells were harvested by centrifugation (5 min at 4,000 ×*g*) from 40 L of algal culture and the resultant cell pellet was resuspended into 10 mM sodium phosphate buffer (pH 7.5) with 0.25 M sucrose and protease inhibitor cocktail (ProteoGuard™ EDTA-free protease inhibitor cocktail, Clontech, CA, USA). The cells were placed on ice for 15 min and then broken by a French Press with 0.8 kpsi at 4 ℃. To remove some debris, cell lysates were centrifuged at 3,000 ×*g* for 10 min at 4 ℃. After centrifugation, a large amount of LBs was obtained in the supernatant fraction, called post-nuclear supernatant (PNS), as described in the Nature protocol (Ding et al., 2013). Sucrose concentration in the PNS sample was adjusted to 1 M. Then, the sample was applied to a centrifuge tube containing layers of 1.2, 1.0, 0.8, 0.5, 0.25 and 0 M sucrose for a sucrose stepwise gradient centrifugation for 30 min at 10,000 ×*g* (SW40 Ti rotor, Beckman Coulter, CA, USA) at 4 ℃. LBs fractionated onto the top layer was carefully collected by a pipette and then transferred to a new 1.5 mL Eppendorf tube. The crude LB fraction was washed three times with 10 mM sodium phosphate buffer (pH 7.5) followed by centrifugation for 10 min at 10,000 ×*g* at the bottom (12,000 rpm using TMP-21 rotor of TOMY MX-201 and a ARO15-24 of TOMY MX-307 Mini-

refrigerator centrifuge, TOMY, Japan) to remove contaminants of other organelles, cytosolic proteins and other materials.

2.3 BODIPY staining

BODIPY (493/503, Life Technologies, CA, USA) stock solution was prepared as 1 mg/mL in dimethyl sulfoxide. The staining was carried out by mixing with algal culture or isolated LBs in order to observe LBs in the living cells under a fluorescent microscope (BX50, Olympus, Japan).

2.4 Analysis of lipid composition in LBs

The extraction of lipids was performed by following a previous protocol (Katavic et al., 2006). Extracted neutral lipids and methyl-esterified polar lipids were detected by an FID-equipped capillary gas chromatograph (GC-2014AFSC; Shimadzu, Kyoto, Japan) with a CP-SIL 5CB column (50 m, 0.32 mm I.D., 0.12 μm; Agilent, Santa Clara, CA, USA). The carrier gas used was He with a flow rate of 2.08 mL/min in split-less mode. The column temperature was set to 60 ℃ for 1.5 min, heated at a speed of 20 ℃/min to 130 ℃, and then taken at 4 ℃ min^{-1} to 300 ℃, and holding at 300 ℃ for 25 min.

Then composition of unknown peaks were analyzed by gas-chromatograph, GC-2010, equipped with a mass spectrometer, QP-2010 (Shimadzu, Kyoto, Japan) by following our previous method (Kotajima et al., 2014). I identified these unknown peaks from the retention times and mass spectrums by using similarity search. Five μg heptadecanoic acid (17:0) and n-toriacontane (C_{30}) dissolved in hexane was added to each sample as internal standard (IST).

2.5 Protein extraction

The proteins of isolated LBs were extracted using two methods. One method involved treatment with 90% acetone (Wako, proteomics grade, Osaka, Japan) for 16 h followed by centrifugation for 10 min at 12,000×*g* (15,000 rpm; TMP-21 rotor of TOMY MX-201 and a ARO15-24 of TOMY MX-307 Mini-refrigerator centrifuge,

TOMY, Tokyo, Japan). After discarding the supernatant, precipitated proteins were treated with 90% acetone for another 16 h (preparation: AB1). The other method involved treatment with petroleum ether according to the methods of Katavic *et al*. (Katavic et al., 2006) in which neutral lipids and polar lipids were extracted first (preparation: AB2).

PNS samples were prepared from cells grown under N-deficient conditions (PNS/-N) and N-sufficient (standard) conditions (PNS/+N as control). Proteins were prepared from both PNS samples by 90% acetone precipitation and petroleum ether, according to the method described above.

Precipitated proteins were dissolved in lysis buffer con-taining thiourea and tris (LB-TT) [7 M (w/v) urea, 2 M (w/v) thiourea, 4% (w/v) CHAPS, 18 mM (w/v) Tris-HCl pH 8.0, 14 mM (w/v) Trizma base, 0.2% (v/v) triton X-100, 50 mM (w/v) DTT, 1% (v/v) pH 3-10 ampholyte, and two EDTA-free proteinase inhibitor (Roche Diagnostics GmbH, Tokyo, Japan), 1% (v/v) pharmalyte pH 3–10 and 50 mM DTT] (Agrawal et al., 2011). Proteins were denatured by adding a SDS-containing sample buffer containing 62 mM Tris pH 6.8, 10% (v/v) glycerol, 2.5% (w/v) SDS, 5% (v/v) 2-mercaptoethanol (pH 6.8 with HCl) and 0.004% bromophenol blue [sample/buffer = 1/1 (v/v)] at 65 ℃ for 10 min. Proteins were analyzed by SDS–PAGE on 12.5% gel (w/v) and visualized using OLEO™ fluorescent gel stain (Bio-Rad Laboratories, Inc., CA, USA). The protein concentration of samples for SDS-PAGE was determined by the Bradford Assay (Bio-Rad).

2.6 Western blotting

Western blot analysis was carried out by following a previous protocol (Tsuji et al., 2012). Briefly, proteins on a SDS-PAGE gel were transferred to a PVDF membrane using semi-dry transfer apparatus (Bio-Rad). The membrane was blocked by treating with Blocking One reagent (Nacalai Tesque Co. Ltd, Kyoto, Japan) over night at 4 ℃. This pre-treated membrane was probed for testing immune-reactivity with anti-ribulose-1,5-bisphosphate carboxylase/oxygenase (RuBisCO) large subunit (LSU) antibody (Catalog AS03 037-10, Agrisera, Vännäs, Sweden). This was followed by

washing the membrane with TBS-Tween [50 mM Tris-HCl pH 8.2, 0.1% (v/v) Tween 20, 150 mM NaCl] for 5 min three times. Finally, the membrane was incubated in a 1:20000 solution of alkaline phosphatase-conjugated anti-goat IgG (Bio-Rad) for 1 h at room temperature. Immunologically positive signals from protein bands were visualized using the CDP-star detection reagent and FUJIFILM ImageQuant LAS 4000 mini (GE Healthcare Bio-Sciences KK, Tokyo, Japan).

2.7 Protein database construction

The Trinity platform for constructing the *T. lutea* database was used by referring a previous study (Haas et al., 2013). To complete protein database, I assembled transcriptomic data (SRR824147) (Carrier et al., 2014) obtained from DDBJ (http://trace.ddbj.nig.ac.jp/DRASearch/) by using default Trinity (Garnier et al., 2014) settings. Prior to assembly preprocessing of transcriptomic data was done with FASTX Toolkit (http://hannonlab.csh1.edu/fastx_toolkit/) to remove low quality (Q<20) reads. Then, those assembled RNA sequences were converted to protein sequences using Bio-Perl.

2.8 Mass spectrometry analysis of proteins

LC-MS/MS analyses were conducted as described in our previous study (Fujiwara et al., 2014). Proteins of AB1, AB2 were analyzed, I also excised and analyzed five visible protein bands derived from AB1. Proteins were separated using a ready-made 12.5% (w/v) SDS-polyacrylamide gel (ATTO, Tokyo, Japan) and stained with Flamingo (Bio-Rad). Each lane with several protein bands was sliced into eight pieces of equal length and washed twice with HPLC-grade water containing 60% (v/v) acetonitrile (Kanto Chemical, Tokyo, Japan) and 50 mM ammonium bicarbonate. Then, the gel pieces were incubated in solution with 10 mM DTT and 50 mM ammonium bicarbonate for 45 min at 56℃, followed by another incubation in 55 mM iodoacetamide and 50 mM ammonium bicarbonate for 30 min at room temperature.

The gels were washed twice with HPLC-grade water containing 60% (v/v) acetonitrile and 50 mM ammonium bicarbonate and dried in a vacuum concentrator.

The dried gel pieces were incubated with 2 μL of a 10 ng/μL trypsin (MS grade gold; Promega, Wisconsin, USA) and 50 mM ammonium bicarbonate at 37℃ for 16 h. After transferring digested peptides to a new microfuge tube, the gel was treated twice with 20 μL of 0.2% (v/v) formic acid (Wako, Tokyo, Japan) and 50% (v/v) acetonitrile, and then all extracted peptides were collected and combined in to a new microfuge tube. The extracts were dried in a vacuum concentrator and dissolved into a mixture of 0.1% (v/v) formic acid and 5% (v/v) acetonitrile. The dissolved solution was filtered by the *Ultrafree*-MC *Centrifugal* Filters (PVDF 0.45 μm; Millipore, Massachusetts, USA) to avoid contamination of gel pieces.

LC-MS/MS analyses were performed using the LTQ-Orbitrap XL-HTC-PAL system (Thermo Fisher Scientific, Bremen, Germany). As a sample for analysis, the trypsin digests were loaded onto the column (100 μm internal diameter, 15-cm length; L-Column, CERI) using the Paradigm MS4 HPLC pump (Michrom BioResources, CA, USA) and HTC-PAL autosampler (CTC Analytics, Zwingen, Switzerland), and then eluted by a gradient of 5 to 45% (v/v) acetonitrile in 0.1% (v/v) formic acid for 26 min. The eluted peptides were introduced directly into an LTQ-Orbitrap with a flow rate of 500 nL/min and a spray voltage of 2.0 kV. MS/MS spectra were analyzed by MASCOT server (version 2.4) in house (http://www.matrixscience.com/) and the profiles were compared with those annotated from *T. lutea* transcriptome database according to a recent publication (Carrier et al., 2014). The MASCOT search parameters were as follows: set off the threshold at 0.05 in the ion-score cut off, peptide tolerance at 10 ppm, MS/MS tolerance at ±0.5 Da, peptide charge of 2^+ or 3^+, trypsin as enzyme allowing up to one missed cleavage, carbamidomethylation on cysteine as a fixed modification and oxidation on methionine as a variable modification. In addition, a BLAST (http://www.ncbi.nlm.nih.gov/) database was also used for further detailed analysis as described below.

2.9 BLAST annotation

I used Blast2GO (V 2.7.2) (http://www.blast2go.com/b2ghome) for annotation of peptide sequences (Gotz et al., 2008). As MASCOT search engine analyzes the MS-

MS spectra, it identifies peptide fragments and assigns them to proteins of the constructed *T. leutia* database. I considered the transcript sequences of such identified proteins as complete peptide sequences of the related peptide fragments. These sequences of peptide fragments were submitted to the BLAST Blast2GO java web start for annotation. This software is connected to the BLAST database where similarity searches will be performed for the query sequences. Available annotations and GO (Gene Ontology) terms from the obtained hits were statistically analyzed by Blast2GO and the probable annotations were assigned to the query sequences. The peptide FASTA file with 755 peptide sequences was given as input to Blast2GO. In this tool, I used 'blastp' to search for hits in 'nr' (non-redundant) database to identify at least 100 best alignments with a minimum e-value cutoff of $1.0e^{-3}$ and annotation parameters like GO-weight cutoff and Annotation threshold parameters were set to default (GO-weight=5; Annotation threshold=55). All query peptide sequences with BLAST hits were assigned with a description which is the most probable function of the detected hits. I also performed InterProScan available in the tool, to allow annotation based on their domain information. This was followed by mapping of functional information using GO data of the identified BLAST hits. The process of assigning functional terms to query sequences from the pool of GO terms gathered in the mapping step is based on the gene ontology vocabulary. The algorithm computes annotation score basing on quality of GO assignments and evidence code. Finally, annotations were assigned for those sequences which qualify the threshold value (Conesa and Götz, 2008). These annotations are presented along with their peptide MASCOT results. Further, I selected most abundant peptide sequences from each sample based on their MASCOT score if Mol% is more than 1%. Thus a total of 70 abundant peptides were re-analyzed for their annotations using Blast2GO with same settings. Peptide sequences without any Blast hits were left unannotated.

3 Results

3.1 Algal growth and microscopic observation of LBs

The change in intact cells of LBs was carefully observed under fluorescent

microscope when *T. lutea* cells were initiated to grow in N-sufficient medium (final concentration of nitrate: 1.4 mM) in a batch culture (Fig. 2). However, it was found that the nitrate concentration decreased and finally depleted after approximately 9 days at the early stationary phase in separate experiments. LBs commonly observed as BODIPY-stained neutral lipid particles in intact cells were very tiny at the logarithmic growth phase and became more obvious when growth stage proceeded close to the stationary growth phases after 10 days (Fig. 2).

When the stationary growth phase cells at day 17, they were transferred to fresh -N medium, the size of LBs were becaming obviously larger and larger while chlorophyll fluorescence started to decay (Fig. 3, Fig. 4). In *T. lutea*, it seems that the LBs remained as individual entities without fusing with each other, but appeared to be one large LB because of overlapped images under the microscope (Fig. 4, Fig. 5). This feature is different from the LBs of the unicellular green alga *Chlorella* in which large-sized LB was largely formed by fusion of several LBs in the cell (Lin et al., 2012). LBs of *Chlorella* mainly contains TAG, but biochemical analysis of whole cellular lipids in *T. lutea* cells showed high content of alkenones (Sukenik and Wahnon, 1991; Brown et al., 1993; Liu and Lin, 2001). Owing to the difference in the components of lipid molecules and proteins present in *T. lutea* LBs, such difference in LB formation may also be observed.

3.2 Isolating LBs from *T. lutea*

In this study, I established a modified method for LB isolation from the haptophyte *T. lutea* (Fig. 5A). After the French Press treatment for breaking the cells, nuclear contamination was removed by a low speed centrifugation to obtain the PNS. In the PNS fraction a large number of round-shaped BODIPY-stained vesicles, namely isolated LBs, were clearly observed, but some contamination of broken cell debris was also observed (Fig. 5B and C).

Next, the PNS fraction was applied to a sucrose density gradient centrifugation with six stepwise density-layers of sucrose (see Materials and Methods section). All the visible debris and membranes of broken cells were separated into the respective layers.

When the fraction of each layer was carefully observed under the microscope, most LBs were found to be floating in the fraction on top of the most upper layer (Fig. 6). As PNS suspended in 1 M sucrose was applied to 1 M sucrose layer (the second layer from the bottom in Fig. 6A), some debris attached to LBs could be removed during floating through several sucrose layers.

Microscopic images of BODIPY-stained purified LBs under both bright field and fluorescence microscopes showed no obvious contamination of chloroplasts in the obtained LB fraction (Fig. 7A and B). Repeatability of this method for isolating LBs was confirmed by microscopic observations in additional experiments (Fig. 8). These results show that the purified LBs isolated from *T. lutea* are composed of neutral lipids and commonly spherical in shape with a size ranging from 0.1 to 2 μm in diameter.

3.3 Lipid analysis of LBs in *T. lutea*

In this study, components of the purified LBs of *T. lutea* were firstly analyzed by GC-FID, and three repeated analyses showed the presence of long-chain alkenones (mainly C_{37} and C_{38}) as major component (average content of total lipids: 74.2%), long-chain alkenes (1.2%), and others (24.6%) (Table 1, Fig. 9, Table 2). Fatty acids were negligible, suggesting that they were below the sensitivity of detection by both GC-FID and GC-MS, compared with the amount of LBs used for neutral lipids analysis. Based on these results, it can be inferred that LBs in Isochrysidales *T. lutea* (Haptophyte) may bettr be called as the "alkenone body (hereafter, AB)". Thus ABs may serve as a storage center for neutral lipids in *T. lutea* cells since the present results are in close accordance with the function of LBs described in a previous report on *I. galbana* and *E. huxleyi* (Eltgroth et al., 2005). The recovery rates of alkenones during the isolation and purification process of ABs from 40-L culture cells were 0.027 - 0.11% in two separate experiments. Isolation efficiency of ABs from whole cells was very low since the loss of ABs was quite high during the process of cell disruption.

3.4 SDS-PAGE and Western blot analysis of AB proteins in *T. lutea*

Properties of LBs, especially the contents of proteins and lipids in their amounts and

categories, have been reported to vary considerably among algal species (Eltgroth et al., 2005; Murphy et al., 2009; Wang et al., 2009). It was also documented that the methods used for protein extraction would affect the protein amount in sugarcane (Amalraj et al., 2010). As no generally applicable method is available for different organisms, I decided to develop a new method by modification of previously reported methods that could be potentially applicable for the extraction of LB proteins from alkenone-producing algae.

I compared two methods for extracting lipids from ABs of *T. lutea* in order to obtain proteins from purified LBs and a well-resolved SDS-PAGE profile therein. Two kinds of organic solvents, namely 90% acetone and petroleum ether were used for preparing the AB1 and AB2 samples, respectively (Fig. 7C). Even on SDS-PAGE in which high amount of proteins (ca. 3 μg and 2 μg for AB1 and AB2, respectively) was applied on each lane, AB1 produced clearer protein bands in comparison with AB2. This result further suggests that acetone is better than petroleum ether as organic solvent for removing lipids and preparing pure proteins for use in downstream proteomic analysis.

In the control (PNS of N-sufficient cells, PNS/+N), Rubisco (55 kDa) was abundantly seen, whereas no such clear band was observed in the PNS of N-deficient cells (PNS/-N) (Fig. 7C). These results apparently indicate that cells grown in N-deficient medium are more suitable for isolating LB because of the low content of proteins that might serve as contaminants, and are similar to those in a previously reported study on *Chlamydomonas* (Moellering and Benning, 2010). There also are difference in both high and low molecular mass of proteins between PNS/+N and PNS/-N. This may be due to down regulation of those proteins under long time nitrogen depletion (Garnier et al., 2014).

Western blot analysis with anti- ribulose-1,5-bisphosphate carboxylase/oxygenase antibody showed that ABs purified from PNS/-N contained no contamination of this chloroplast-located major protein, indicating that LBs were well purified (Fig. 7D). The purity of LBs was further demonstrated by calculating proteins/alkenones ratio in PNS and isolated LBs fractions since alkenones are the main component of lipid bodies (therefore named as ABs) in *T. lutea* (see Table 1). The ratio of proteins/alkenones in

ABs decreased to 1/5-1/7 times lower values in comparison with that in PNS (crude extracts) in two separate experiments.

Therefore, N-deficient cell culture approach works not only to increase neutral lipid contents, but also to reduce chloroplastic proteins. The present results confirmed the previous study reporting that better isolation quality of LBs was obtained in the cells grown under N-deficient conditions than that from control (Moellering and Benning, 2010).

3.5 Proteomics of ABs from *T. lutea*

Protein composition of the two purified AB samples, namely AB1 and AB2, isolated from *T. lutea* was determined by LC-MS/MS analyses (see Materials and Methods section). Annotated lists of matched proteins were compiled and ranked by their relative abundance based on exponentially modified protein abundance index (emPAI). The parameter Mol%, calculated by the equation of $[(\text{emPAI})/\Sigma(\text{emPAI})] \times 100\%$, represents the protein abundance in each subcellular fraction (Ishihama et al., 2005; Baba et al., 2011). Identification of AB proteins of *T. lutea* was determined by searching the highest sequence similarity in the database using BLAST search. Peptide sequences obtained from the LC-MS/MS analysis were also compared to the *T. lutea* protein database for finding proteins matched in identity.

In these proteomic analyses I identified many proteins, but I mainly focus my discussion on the identified proteins with a Mol% over 1%. In AB1, a total number of 514 protein sequences were annotated. Among them, the top 18 hypothetically annotated proteins are listed in Table 3. The top 5 hypothetical functions annotated in AB1 (with number of reads in parenthesis) were proton pumps (V-ATPase) (5), cytoskeletons (2), transferases (1), energy metabolisms (1) and photosystem II (1) (shown diagramatically in Fig. 10A). Similarly, 186 protein sequences were identified in AB2 (Table 4).

The proteins matched with the highest Mol% were quite similar in both AB1 and AB2. Among these, V-type H^+-ATPase (V-ATPase) appeared as the most abundant protein. The Mol% values were 6.4% and 9.4% in V_1 sector subunit A, 5.7% and 5.1%

in B, 10.1% and 7.3% in E and 1.9% and 2.4% in V_0 sector subunit d in AB1 and AB2, respectively (Table 3, Table 4). The abundant proteins identified in both AB samples of *T. lutea*, such as proton pump (V-ATPase), energy metabolism (ATPase), may possibly have some important functions during the formation and development of ABs.

The other abundant proteins comprise a hypothetical protein EMIHUDRAFT_465517 (5.8% and 2.6%), SPFH domain-containing protein (4.1% and 2.7%) and coccolith scale associated protein-1 (1.5% and 2.5%), FAD-dependent pyridine nucleotide-disulfide oxidoreductase (1.2% in both), phosphate ABC transporter substrate-binding protein (1.4% and 1.6%) and outer mitochondrial membrane protein porin (1.8% and 1.2%) in AB1 and AB2, respectively (Tables 3-4). In addition, actin, short-chain dehydrogenase reductase SDR and ATP synthase were also detected.

Some other proteins identified in the samples also include cycloartenol-c-24-methyltransferase 1-like protein (3.1%) in AB1 and mitochondrial phosphate carrier protein (1.3%), histone h3 type 2 (3.5%) and histone h2b (1.9%) in AB2. (Tables 3-4, Fig. 10). Despite a high level of purity of the studied ABs, some proteins, such as the light harvesting protein which is more closely related to PSII, was identified. It likely suggests some contamination of proteins present in the tested AB samples.

As visible protein bands were detected in the AB1 protein sample (Fig. 7C), I wanted to know what these proteins are and to re-confirm the major proteins existing in ABs. Therefore, in an independent experiment, I excised and analyzed five specific bands cut out from SDS-PAGE gel to obtain more information on proteins over the slice analysis. The five major bands with molecular masses (kDa) of 84.2, 66.7, 55.3, 37.1 and 33.0 (AB1 in Fig. 7C) were separately brought to proteomic analysis.

According to the similarity search of sequenced peptides in database (Table 5), various subunits of V-ATPase were identified predominantly in three bands with molecular masses of 66.7, 55.3, and 33.0 kDa. Further, both a phosphate ABC transporter substrate-binding protein and a hypothetical protein EMIHUDRAFT_465517 were dominantly identified in the 84.2 kDa band. In the 37.1 kDa band, a cyclocartenol-*c*-24-methyltransferase 1-like protein, expected to be an

enzyme belonging to a family of sterol 24-C-methyltransferases that performs distinctive activity in transferring C_1-residue, was identified as the dominant protein (Table 5). Functional category of the proteins is briefly summarized in Figure 10B.

4 Discussion

4.1 Isolation of ABs from *T. lutea*

The cell structures of the secondary symbiotic algal species such as is generally known to be very different from those of the primary symbiotic algae. In *T. lutea* the cell commonly has four layers of chloroplast envelopes with an ER membrane at the outmost position. Therefore, isolation of LBs would be much more difficult in the secondary symbiotic algae such as haptophytes in comparison with the primary symbiotic algae such as green algae and higher plants.

The isolation of LBs was previously reported in the haptophyte *I. galbana* CCMP 1323, unicellular green microalgae such as *Chlamydomonas* and *Chlorella* in microalgae and in plants as well (Eltgroth et al., 2005; Katavic et al., 2006; Nguyen et al., 2011; Lin et al., 2012; Horn et al., 2013). By replicating the methods described in the previous reports, I attempted to isolate the ABs from *T. lutea* several times, but were not successful in obtaining better quality ABs, primarily because of chloroplast contamination. Such failure may be due to different lipid contents, varying cell properties or morphology of LBs in each species. Even though *T. lutea* is a sister taxon of *I. galbana*, some differences in their lipid contents and profiles as well are also expected. I list the methods used in previous studies for LB isolation from various organisms and also describe some possible causes of failure in my experiments with *T. lutea* for further argument although the exact reasons are not fully known (Table 6).

Three important points for the successful isolation and purification of ABs of *T. lutea* in this study. The first point relates to the preparation of very large AB-harboring cells that were obtained by maintaining cells under -N conditions for 16 days (Fig. 3). This condition was used since LBs are generally known to be enlarged under -N conditions in other taxonomically different microalgae (Horn et al., 2013; Nojima et al., 2013; Pribyl et al., 2013) as well as in haptophytes *I. galbana* and *T. lutea* (Eltgroth et al.,

2005; Garnier et al., 2014). Additionally, N-deficient culture was also effective in decreasing RuBisCO contamination in AB fraction since chloroplasts were degraded during incubation as confirmed by the absence of chlorophyll auto-fluorescence under fluorescent microscope (red fluorescence in Fig. 3, Fig. 4).

The second important strategy for isolation of ABs was an improvement of the cell disruption method. Initially, I tested many kinds of cell disruption methods, such as the Yeda press connected to a compressed nitrogen gas cylinder, sonication, grinding by motor and pestle under liquid nitrogen and a French Press., but the results were not ideal. After tens of repeated experiments, finally I found that the French Press was the best method for *T. lutea* cell disruption based on the efficiency of recovery and purity of ABs isolated. Using this method, the high amount of ABs was easily obtained as a lipid body pat on top of the layer following sucrose density gradient centrifugation (Fig. 6).

The third point is related to the sucrose gradient step, and involved using six different sucrose density layers in my experiment in order to enhance the washing effect and remove all visible debris and membranes derived from broken cells. Therefore, ABs were effectively separated as the "alkenone body layer" floating onto the top of the centrifuge tube and purified by removal of attached materials on AB surface during passing through several sucrose layers (Figure 6A).

4.2 The AB proteins of *T. lutea*

There are different types of LBs in plant seeds and leaves (Jolivet et al., 2013). V-type H^+-ATPase was detected as major component of LBs in leaves of TAG-producing higher plants such as *Arabidopsis* (Shimada et al., 2014) and mesocarp tissue of avocado (Horn et al., 2013). However, the protein V-ATPase has not been found in seed LBs until now. Interestingly, V-ATPase has been identified from *T. lutea* cells cultured under N-deficient conditions (Song et al., 2013). The V_1 subunit of V-ATPase is known to be responsible for ATP hydrolysis, whereas V_0 subunit for transporting H^+ across the membrane (Marshansky and Futai, 2008). Although, V-ATPase is localized in the tonoplast (vacuolar membrane), Golgi apparatus and in other coated vesicles in

eukaryotes, the subunit V_0 is typically localized in the ER membrane where the whole molecule of V-ATPase is assembled (Bauerle et al., 1993; Kane et al., 1999; Marshansky and Futai, 2008; Lee et al., 2010; Viotti et al., 2013).

It was reported that the haptophyte *E. huxleyi*, a sister taxon of *T. lutea*, produces alkenones by associating with internal organelles such as the ER and the coccolith-producing compartment (Sawada and Shiraiwa, 2004). The coccolith-producing compartment is thought to contain V-ATPase exporting protons for calcification, and is known to be formed by budding from the Golgi body whose membrane is closely associated with ER (Kane et al., 1999; Corstjens and Gonzalez, 2004). According to the ultrastructure analysis of LB formation in *T. lutea*, it was realized that LBs were always observed to appear by attaching closely to the outer membrane of ER (Liu and Lin, 2001). It was also reported that a g6574 protein identified by proteomics study of LB in the oleaginous diatom *Fistulifera solaris* exist in both ER and LBs (Nojima et al., 2013). As a secondary symbiotic microalga, this diatom also has a four-layered chloroplast envelope, of which the outmost plastid envelope is apparently connected to the outer membrane of ER.

Based on all these known evidence, it seems that the V−ATPase is most likely assembled in ER as the major protein of ABs in *T. lutea*. Therefore, I hypothesize that neutral lipids involving alkenones as the major component are first accumulated in the internal space of ER membranes through the support of V-ATPase located on the outer membrane of ER. Following the accumulation of neutral lipids in the vicinity, the budding of ABs from ER might be promoted, as modeled in Figure 11. As ABs observed in the logarithmic growth phase were very small and clearly enlarged during the cell growth stage (Fig. 2), it seems that alkenones are also needed to be transported through the AB membrane.

Another point is, in *Chlamydomonas* V-ATPase was suggested to be related with contractile vacuole (Conesa and Götz, 2008), but the formation and ultrastructure of vacuole looks very similar to lipid bodies (Peters et al., 2001). Besides, there is no information on *T. lutea* whether they have vacuole or not. There is a possibility that the origin of lipid bodies is vacuole, during evolution their function or structure become

modified and then completely become lipid bodies. Or the vacuole is still exist in *T. lutea* cells, but lipid bodies is another branch of vacuole. Further studies needs be studied on this part.

Homologous protein of the hypothetical protein EMIHUDRAFT_465517 was found only in haptophytes by BLAST search in NCBI. Moreover, those sequences were quite similar among alkenone producers which are limited only to the haptophytes in BLAST homolog search by using protein database in Marine Microbial Eukaryote Transcriptome Sequencing Project (http://camera.calit2.net/mmetsp/combinedassemblies.php) (Table 7). It is tempting to suggest that the hypothetical protein EMIHUDRAFT_465517 is related to alkenone production or metabolism.

The SPFH domain-containing protein was previously found in the plasma membrane, Golgi apparatus, lipid droplets, mitochondria, and ER (Langhorst et al., 2005; Morrow and Parton, 2005; Browman et al., 2006). It has been suggested that this protein is possibly involved in lipid raft and membrane microdomains (Browman et al., 2007), but the molecular basis of its function remains unknown. The SPFH domain-containing protein located in the ER membrane may be involved in LBs, especially during the process of budding of LBs, as suggested in Figure. 11.

In my study, a coccolith scale associated protein-1 was also identified as one of the AB-associated proteins in alkenone-producing but not in non-coccolith-producing haptophytes (Tables 3-4). This result is supported by the evidence that alkenones are localized in the coccolith-producing compartment in the coccolithophore *E. huxleyi* (Sawada and Shiraiwa, 2004) and by a previous study that observed the increase in the relative abundance of the protein over six times under N-depletion conditions (Garnier et al., 2014). It is worth to note, however, in the diatom *Phaeodactylum tricornutum*, this protein (AB537972.1 from the TAG-producing but non-alkenone-producing coccolithophore *Pleurochrysis carterae*) was also found as the most up−regulated protein under N-depletion (Valenzuela et al., 2012). Although function of this protein in *T. lutea* remains unknown, its identification from the ABs likely indicates a contribution towards LB or AB formation in the secondary symbiotic marine

microalgae.

I also identified a mitochondrial ATP synthase with low Mol% (1.1%) and emPAI (3.7) values, which was likely involved in energy metabolism pathways in accordance with the results in a land plant *Arabidopsis* (Shimada et al., 2014) and a marine coral-dinoflagellate endosymbiotic microalga (Peng et al., 2011). A cycloartenol-*c*-24-methyltransferase 1-like protein was also identified, and this enzyme is known to be associated with steroid biosynthesis in higher plants such as soybean (Song and Nes, 2007). A novel AB protein short-chain dehydrogenase reductase SDR detected previously in *Brassica napus* (Katavic et al., 2006) was suggested to have a possibly unknown function in LB structure, synthesis or degradation. In microalgae, the presence of brassicasterol and epigrassicasterol was confirmed in chromophyte algae such as diatoms and haptophytes including *Tisochrysis lutea* (Gladu et al., 1990). The enzyme *S*-adenosyl-L-methionine–cycloartenol methyltransferase activity was determined in green microalgae such as *Trebouxia* sp. and *Scenedesmus obliquus* (Wojciech.Za et al., 1973). However, the connection of this protein to alkenone metabolism remains to be clarified. The co-existence of these metabolites and proteins likely suggests that ABs represent not only just a lipid storage vesicle but also a location for lipid metabolism.

Actin protein identified in my study was determined to have cytoskeleton function. This protein has been detected previously in LB proteins of many species (Peng et al., 2011; Horn et al., 2013; Shimada et al., 2014). Though it was thought to be specific to LBs (Peng et al., 2011), it is still unclear whether it has a function in LBs or appears just as a contaminant. Histone protein has been previously suggested to be associated with LBs before transfer to nuclei during development (Cermelli et al., 2006; Peng et al., 2011).

I also detected some minor proteins which may be involved in lipid metabolism in *T. lutea*. Those proteins are long chain acyl-CoA synthetase which binds fatty acid to produce fatty acyl-CoA, cyclopropane-fatty-acyl-phospholipid synthase, malate dehydrogenase and glycerol-3-phosphate dehydrogenase. These proteins were also reported in *Chlamydomonas* (Nguyen et al., 2011) along with additional proteins that

are involved in acyl-lipid metabolism. This difference may be due to divergence in the species.

Finally, I would like to discuss on the uniqueness of the AB proteome based on my current knowledge of the proteins cataloged in this study. Unlike those in higher plants (Naested et al., 2000; Lin et al., 2002; Siloto et al., 2006), *C. reinhardtii* (Moellering and Benning, 2010; Nguyen et al., 2011) and other microalgae (Peled et al., 2011; Davidi et al., 2012; Lin et al., 2012; Vieler et al., 2012), I did not find oleosin, MLDP, HOSP or LDSP in ABs of *T. lutea* (Tables 3-5). This result may be due to their phylogenetic difference. Therefore, it can be assumed that the V-ATPase in ABs may also function as structural protein which is similar to oleosin or MLDP in the LB since V-ATPase is largely contained as the major protein of ABs in *T. lutea*. To prove this hypothesis, generating antibodies against the V-ATPase subunit A and the hypothetical protein EMIHUDRAFT 465517 will be very useful to confirm the localization of these two proteins by immune-electron microscopy. Furthermore, it will be important to examine the expression of the genes encoding for these abundant proteins in order to reveal their possible metabolic pathways, in future studies.

5 Conclusions

My present study in the alkenone-producing haptophyte *T. lutea* fulfilled the two main objectives, i) establishment of a method to isolate ABs, and ii) providing a significant lipid content and proteome dataset of the ABs. Proteomic analyses revealed V-ATPase as a major protein in ABs of *T. lutea*, and the inventory of identified proteins along with qPCR result of SPFH domain-containing protein gene expression level suggested suggested that the ABs might be derived from the ER. Furthermore, I speculate that the abundant hypothetical protein EMIHUDRAFT 465517 might be strongly related with alkenone metabolism since the ABs dominantly contains alkenones and gene expression level. qPCR results showed that V-ATPase, cycloartenol-c-24-methyltransferase and coccolith scale associated protein-1 were very likely to located on alkenone bodies. Future studies investigating these claims will provide valuable information for elucidating the mechanism of alkenone production in

haptophytes. In addition, a deeper investigation will be required to reveal the whole process of LB formation in *T. lutea*.

Tables and Figures

Table 1. Composition of neutral lipids in purified LBs isolated from N-starved cells of haptophyte *T. lutea*. Each fraction applied for GC-MS analysis was prepared by fractiontion with different organic solvents as described in **Materials and Methods**. Experiments were repeated three times for whole process of algal growth, AB isolation/purification, lipid extraction and GC analysis of lipids.

	Percentage (%) of total neutral lipids		
Sample no.	**Alkenone (%)**	**Alkene (%)**	**Others (%)**
LB-a	70.9	1.4	27.7
LB-b	74.2	1.0	24.8
LB-c	77.6	1.2	21.2
Average	74.2	1.2	24.6

Table 2. List of Peak 1-16 from **Figure 9**.

Peak no.	Percentage (%)			Results of similarity search	Category
	a	b	c		
1	2.0	0.5	0.1	Tetradecan ($C_{14}H_{30}$)	alkane
2	2.1	7.3	4.5	Methyl myristate ($C_{15}H_{30}O_2$)[a]	Fatty acid methyl ester
3	2.2	0.4	0.2	Hexadecan ($C_{16}H_{34}$)	alkane
4	2.3	4.7	4.8	Methyl hexadecanoate ($C_{17}H_{34}O_2$)[a]	Fatty acid methyl ester
5	0.9	0.0	0.4	Methyl heptadecanoate ($C_{18}H_{36}O_2$)[a]	Fatty acid methyl ester
6	0.6	4.7	7.5	Methyl olate ($C_{19}H_{36}O_2$)[a]	Fatty acid methyl ester
7	4.0	1.1	0.5	Ergosta triene	Phytostanols
8	0.5	0.4	0.0	Nanocosane ($C_{29}H_{60}$)	alkane
9	1.9	0.7	0.4	Ergosta triene	Phytostanols
10	2.1	1.0	0.3	Ergosta triene	Phytostanols
11	7.3	3.6	1.9	Ergosta triene	Phytostanols
12	0.9	0.5	0.8	Alkene (C_{31})	Alkene
13	0.5	0.5	0.4	Alkene (C_{31})	Alkene
14	0.7	0.0	0.1	Tocopherol	Phytosterols
15	0.5	0.4	0.3	Ergosterol	Phytosterols
16	0.6	0.5	0.2	Brassicasterol	Phytosterols

a: Identification was performed by comparison with standard.

Table 3. List of top 18 peptides identified by proteomics and database search (mol% ⩾ 1%) in AB1 of the N-deficient cells of haptophyte *T. Lutea*. For SDS-PAGE profile, see **Figure 6C**.

No.	Seq. name	Description	Mass	Score	Mol%	emPAI	Function
1	comp4668_c0_seq1	v-type H^+ ATPase subunit E	26110	729	10.1	33.4	protons pump
2	comp4693_c0_seq1	vacuolar H^+ ATPase A subunit	68574	2758	6.2	20.3	protons pump
3	comp19058_c0_seq1	hypothetical protein EMIHUDRAFT_465517	44412	2605	5.8	19.0	unknown
4	comp16531_c0_seq1	v-type proton ATPase subunit brain isoform	55607	2638	5.7	18.8	protons pump
5	comp16610_c0_seq1	hypersensitive-induced response protein 1/SFPH domain containing protein	34847	730	4.1	13.4	unknown
6	comp16813_c0_seq1	cycloartenol-c-24-methyltransferase 1-like	41374	1413	3.1	10.3	transferase
7	comp17799_c0_seq1	ATPase v_0 complex subunit d	42020	588	1.9	6.1	protons pump
8	comp17371_c0_seq1	outer mitochondrial membrane protein porin	34892	641	1.8	6.0	unknown
9	comp4712_c1_seq3	coccolith scale associated protein-1	74258	1403	1.5	5.1	unknown
10	comp4939_c0_seq1	phosphate ABC transporter substrate-binding protein	99738	2038	1.4	4.5	unknown
11	comp14366_c0_seq2	actin	32986	808	1.2	4.1	cytoskeleton
12	comp4619_c0_seq1	FAD-dependent pyridine nucleotide-disulfide oxidoreductase	47372	1069	1.2	3.9	unknown
13	comp15167_c1_seq1	actin	46230	957	1.1	3.8	cytoskeleton
14	comp16872_c0_seq1	ATP synthase subunit mitochondrial-like	55639	1018	1.1	3.7	energy metabolism
15	comp17302_c0_seq1	short-chain dehydrogenase reductase sdr	39518	926	1.1	3.7	unknown
16	comp13695_c0_seq1	light harvesting protein	8904	93	1.1	3.5	PSII
17	comp18572_c0_seq1	v-type proton ATPase subunit h isoform x2	53790	1120	1.0	3.4	protons pump
18	comp18144_c0_seq1	short-chain dehydrogenase reductase sdr	36841	860	1.0	3.3	unknown

Table 4. List of top 22 peptides identified by proteomics and database search (mol% ⩾ 1%) in AB2 of the N-deficient cells of haptophyte *T. Lutea*. For SDS-PAGE profile, see **Figure 6C**.

No.	Seq. name	Description	Mass	Score	Mol%	emPAI	Function
1	comp4693_c0_seq1	vacuolar H^+ ATPase A subunit	68574	1399	9.4	5.3	protons pump
2	comp4668_c0_seq1	v-type H^+ ATPase subunit E	26110	341	7.3	4.1	protons pump
3	comp16531_c0_seq1	v-type proton ATPase subunit brain isoform	55607	785	5.1	2.9	protons pump
4	comp17087_c0_seq1	histone h3 type 2	16116	50	3.5	2.0	DNA binding
5	comp16610_c0_seq1	hypersensitive-induced response protein 1/SFPH domain containing protein	34847	180	2.7	1.5	unknown
6	comp19058_c0_seq1	hypothetical protein EMIHUDRAFT_465517	44412	483	2.6	1.4	unknown
7	comp4712_c1_seq3	coccolith scale associated protein-1	74258	479	2.5	1.4	unknown
8	comp17799_c0_seq1	ATPase v_0 complex subunit d	42020	183	2.4	1.4	protons pump
9	comp16872_c0_seq1	ATP synthase subunit mitochondrial-like	55639	449	2.1	1.2	energy metabolism
10	comp13695_c0_seq1	light harvesting protein	8904	45	2.0	1.1	PSII
11	comp16982_c0_seq1	ATP synthase F1 subunit alpha	59044	342	1.9	1.1	energy metabolism
12	comp14581_c0_seq2	ATP synthase cf1 alpha subunit	54333	284	1.9	1.1	energy metabolism
13	comp10010_c0_seq1	histone h2b	14429	29	1.9	1.1	DNA binding
14	comp4939_c0_seq1	phosphate ABC transporter substrate-binding protein	99738	680	1.6	0.9	unknown
15	comp15167_c1_seq1	actin	46230	280	1.5	0.9	cytoskeleton
16	comp18572_c0_seq1	v-type proton ATPase subunit h isoform x2	53790	251	1.5	0.8	protons pump
17	comp18677_c0_seq1	v-type proton ATPase subunit d-like	37778	155	1.4	0.8	protons pump
18	comp4690_c0_seq2	mitochondrial phosphate carrier protein	39408	148	1.3	0.7	transporter activity
19	comp4619_c0_seq1	FAD-dependent pyridine nucleotide-disulfide oxidoreductase	47372	432	1.2	0.7	unknown

20	comp17371_c0_seq1	outer mitochondrial membrane protein porin	34892	150	1.2	0.7	unknown
21	comp18144_c0_seq1	short-chain dehydrogenase reductase sdr	36841	122	1.1	0.6	unknown
22	comp18944_c0_seq1	H^+ transporting ATP synthase o subunit	22955	65	1.1	0.6	energy metabolism

Table 5. Identification of top 5 major bands on SDS-PAGE of AB1 of the N-deficient cells of haptophyte *T. lutea* by proteomis and database search (mol% ⩾ 1%). For SDS-PAGE profile, see **Figure 6C**.

No.	Seq. name	Description	Mass	Score	Mol%	emPAI	Function
84.2 kDa							
1	comp4939_c0_seq1	phosphate ABC transporter substrate-binding protein	99738	1509	17.9	4.0	unknown
2	comp19058_c0_seq1	hypothetical protein EMIHUDRAFT_465517	44412	467	13.4	3.0	unknown
3	comp26472_c0_seq1	---NA---	56244	291	4.1	0.9	unknown
4	comp1465224_c0_seq1	---NA---	-	18	4.1	0.9	unknown
5	comp4693_c0_seq1	vacuolar H^+ ATPase a subunit	68574	355	3.6	0.8	protons pump
66.7 kDa							
1	comp4693_c0_seq1	vacuolar H^+ ATPase a subunit	68574	2701	62.9	35.1	protons pump
2	comp4712_c1_seq3	coccolith scale associated protein-1	74258	1713	11.5	6.4	unknown
3	comp19058_c0_seq1	hypothetical protein EMIHUDRAFT_465517	44412	185	1.9	1.1	unknown
4	comp13701_c0_seq1	succinate dehydrogenase	65131	312	1.7	1.0	energy metabolism
5	comp1465224_c0_seq1	---NA---	-	17	1.6	0.9	unknown
55.3 kDa							
1	comp16531_c0_seq1	v-type proton ATPase subunit brain isoform	55607	2386	53.1	42.0	protons pump
2	comp16872_c0_seq1	ATP synthase subunit mitochondrial-like	55639	1117	11.0	8.7	energy metabolism
3	comp16982_c0_seq1	ATP synthase F1 subunit alpha	59044	1261	7.7	6.1	energy metabolism
4	comp14581_c0_seq2	ATP synthase cf1 alpha subunit	54333	481	2.6	2.1	energy metabolism
5	comp19058_c0_seq1	hypothetical protein EMIHUDRAFT_465517	44412	365	1.8	1.4	unknown
37.1kDa							

1	comp16813_c0_seq1	cycloartenol-c-24-methyltransferase 1-like	41374	732	32.6	15.0	transferase
2	comp20854_c0_seq1	saccharopine dehydrogenase	46327	533	6.6	3.1	oxidoreductase activity
3	comp52449_c0_seq1	glutathione s-transferase	41399	526	5.8	2.7	transferase
4	comp20217_c0_seq1	cysteine synthase	41103	353	5.2	2.4	transferase
5	comp18144_c0_seq1	short-chain dehydrogenase reductase sdr	36841	286	4.1	1.9	oxidation-reduction
33 kDa							
1	comp17799_c0_seq1	vacuolar ATPase subunit DVA41	42020	760	14.8	5.5	protons pump
2	comp17302_c0_seq1	short-chain dehydrogenase reductase sdr	39518	469	11.0	4.1	oxidoreductase activity
3	comp21189_c0_seq1	prohibitin	38082	320	9.4	3.5	
4	comp18144_c0_seq1	short-chain dehydrogenase reductase sdr	36841	409	7.8	2.9	oxidoreductase activity
5	comp16610_c0_seq1	SPFH domain-containing protein	34847	205	5.6	2.1	unknown

Table 6. List of previous reports on representative methods for AB isolation and results of adoption of those methods for the isolation of ABs from *T. lutea* in this study.

Literature	Organisms	Methods used	Results in this study on *T. lutea* LB isolation
Eltgroth et al. (2005)	Haptophytes such as *Emiliania huxleyi, Isochrysis galbana* strain "I"	Cells were broken by repeating heating- and thawing-treatments.	ABs could not be released outside of cells. It may be due to insufficinet power for breaking *T. lutea* cells.
Lin et al. (2012)	Unicelluar green alga *Chlorella* sp.	Cells were broken by grinding cells in liquid nitrogen by pestle and mortar.	ABs were not relesed sufficiently from cells by this treatment.
Katavic et al. (2006)	*Brassica napus* (Rapeseed)	Seeds were broken by grinding by a mortar and pestle in a cold grinding medium .	ABs were not relesed sufficiently from cells by this treatment.
Horn et al. (2013)	*Persea americana* (avocado)	Fruits were broken by choping cells with a single-edge razor blade. LBs were separeted from homogenates by ultracentrifuge without sucrose gradient.	Choping tissues/cells was not applicable due to the small size of microalgae. The contamination of chloroplasts could not be removed by ultracentrifuge without sucrose gradient.
Nguyen et al. (2011)	Unicelluar green alga *Chlamydomonas reinhardtii*	Tween-20 was used to wash LBs	Tween-20 was not useful for washing ABs to increase purity since LBs were destroyed.

Table 7. Blast homolog search of Hypothotical protein EMIHUDRAFT_465517 within Haptophyte bioedit local blast

Species	Protein ID	score	E Value
Alkenone producers			
Emiliania huxleyi CCMP370	CAMPEP_0187735904	296	1.00E-80
	CAMPEP_0188184108	264	7.00E-71
	CAMPEP_0193650514	123	2.00E-28
Gephyrocapsa oceanica RCC1303	CAMPEP_0188182174	320	1.00E-87
	CAMPEP_0188165604	271	5.00E-73
Isochrysis galbana CCMP1323	CAMPEP_0193673004	772	0
	CAMPEP_0193682476	545	1.00E-155
No- alkenone producers			
Prymnesium parvum Texomal	CAMPEP_0191215458	150	1.00E-36
Pleurochrysis carterae CCMP645	CAMPEP_0190795772	155	3.00E-38
Pavlova sp. CCMP459	CAMPEP_0190795772	120	6.00E-28
Chrysochromulina polylepis	CAMPEP_0193782362	160	1.00E-39

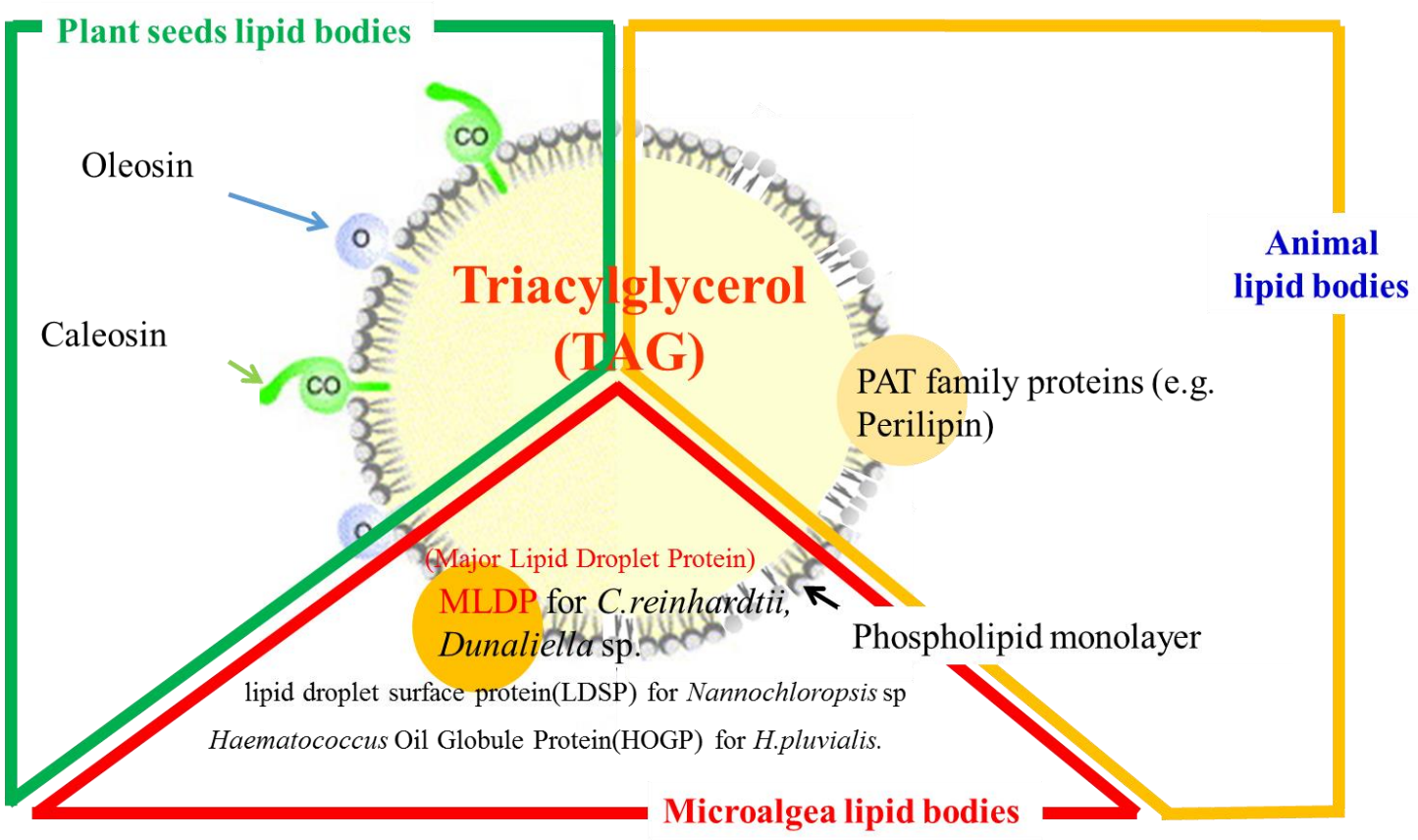

Figure 1. Proteins involved in lipid bodies from animals, plant seeds and microalgae (modified after Moellering and Benning, 2010; James et al., 2011; Vieler, A et al., 2012; Peled, E et al., 2011, Ivo Feussner et al., 2001,)

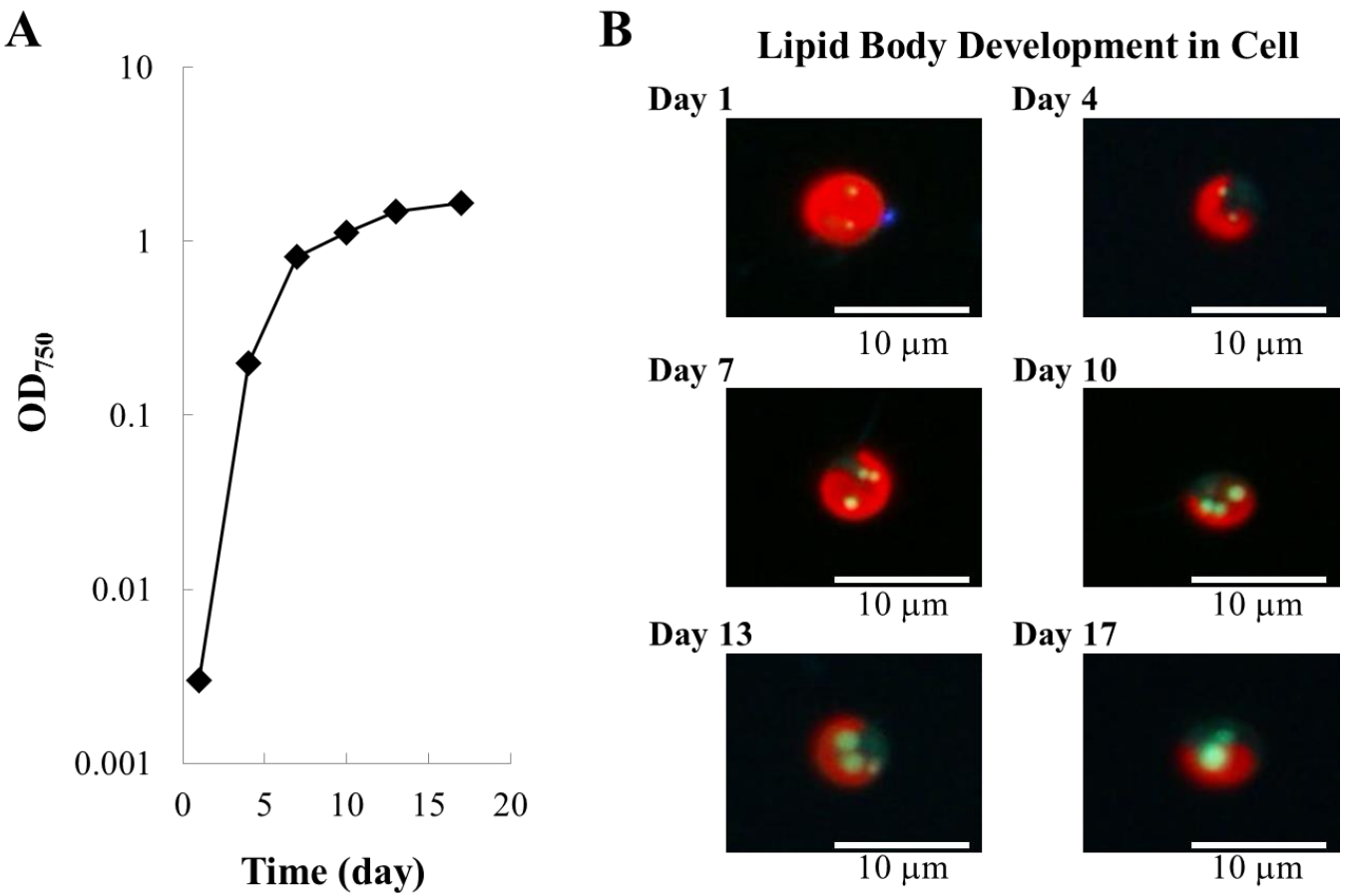

Figure 2. Cell growth curve and AB formation in the batch culture of haptophyte *T. lutea*. (A) Growth curve. (B) Representative pictures of ABs formation during cell growth. Cells were stained with BODIPY 493/503. Cells size, ca. 5 mm in diameter.

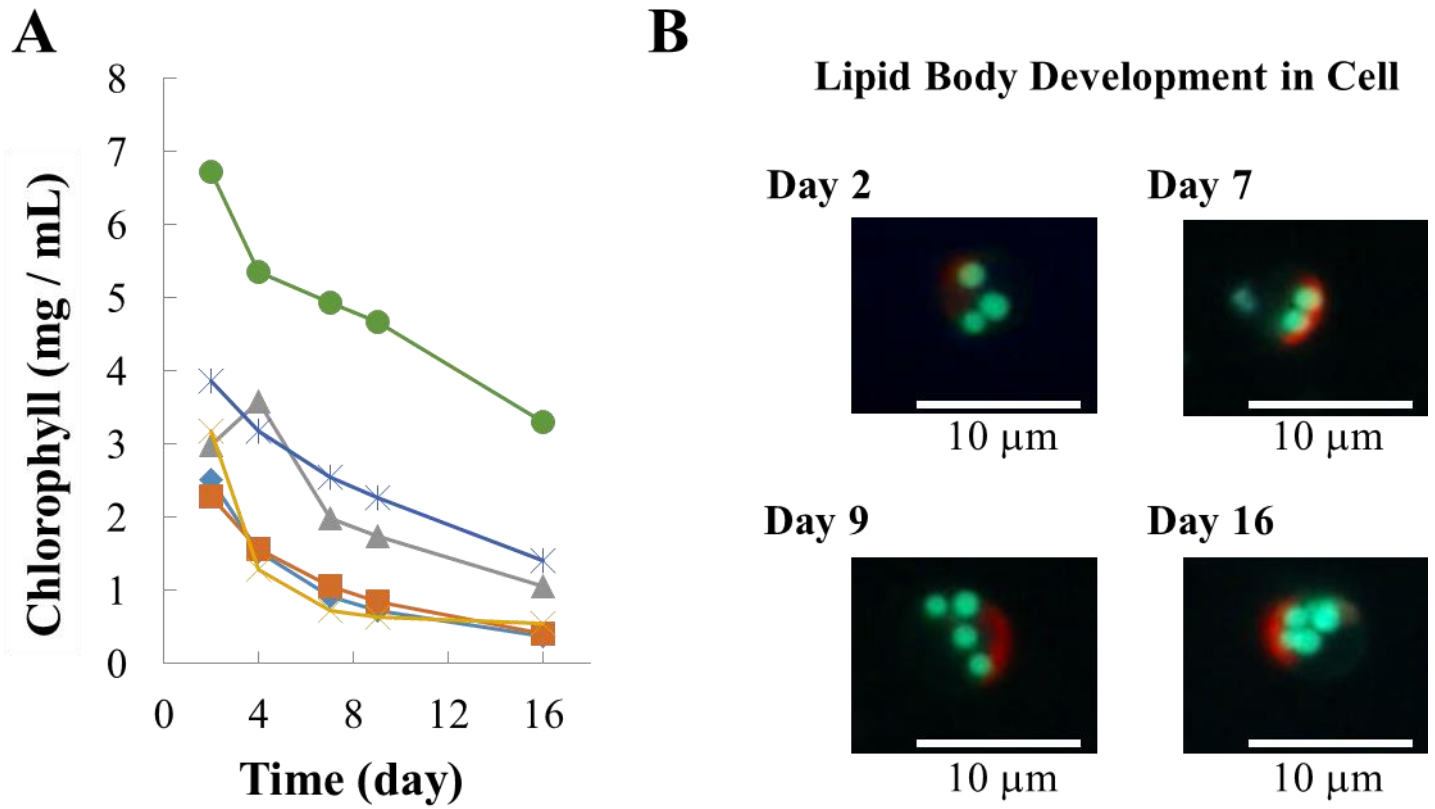

Figure 3. Changes in chlorophyll contents and fluorescent images of ABs after transferring 17-d culture cells into N-deficient medium. (A) Chlorophyll content in six experiments with different cell densities. Symbols indicate the same experimental cultures with different cell density separated into different bottles: bottle 1 (circle), bottle 2 (asterisk), bottle 3 (triangle), bottle 4 (cross), bottle 5 (diamond) and bottle 6 (square). (B) ABs stained by BODIPY 493/503 under fluorescence microscope. Cell size, ca. 5 µm in diameter.

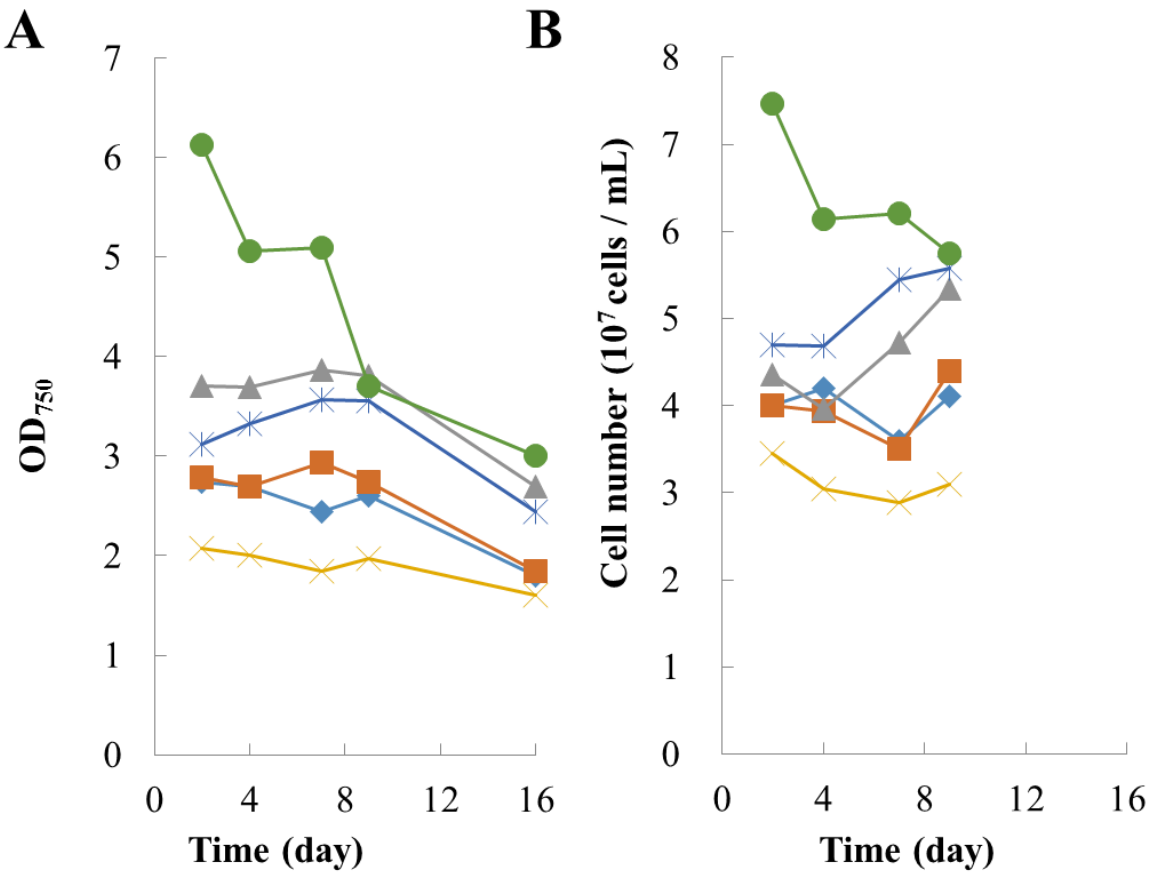

Figure 4. Changes in cell density (A) and cell number (B) during incubation of haptophyte alga *T. lutea* under nitrogen depletion conditions for developing LBs. Symbols indicate the same experimental cultures with different cell density separated into different bottles. Bottle 1 (circle), bottle 2 (asterisk), bottle 3 (triangle), bottle 4 (cross), bottle 5 (diamond) and bottle 6 (square).

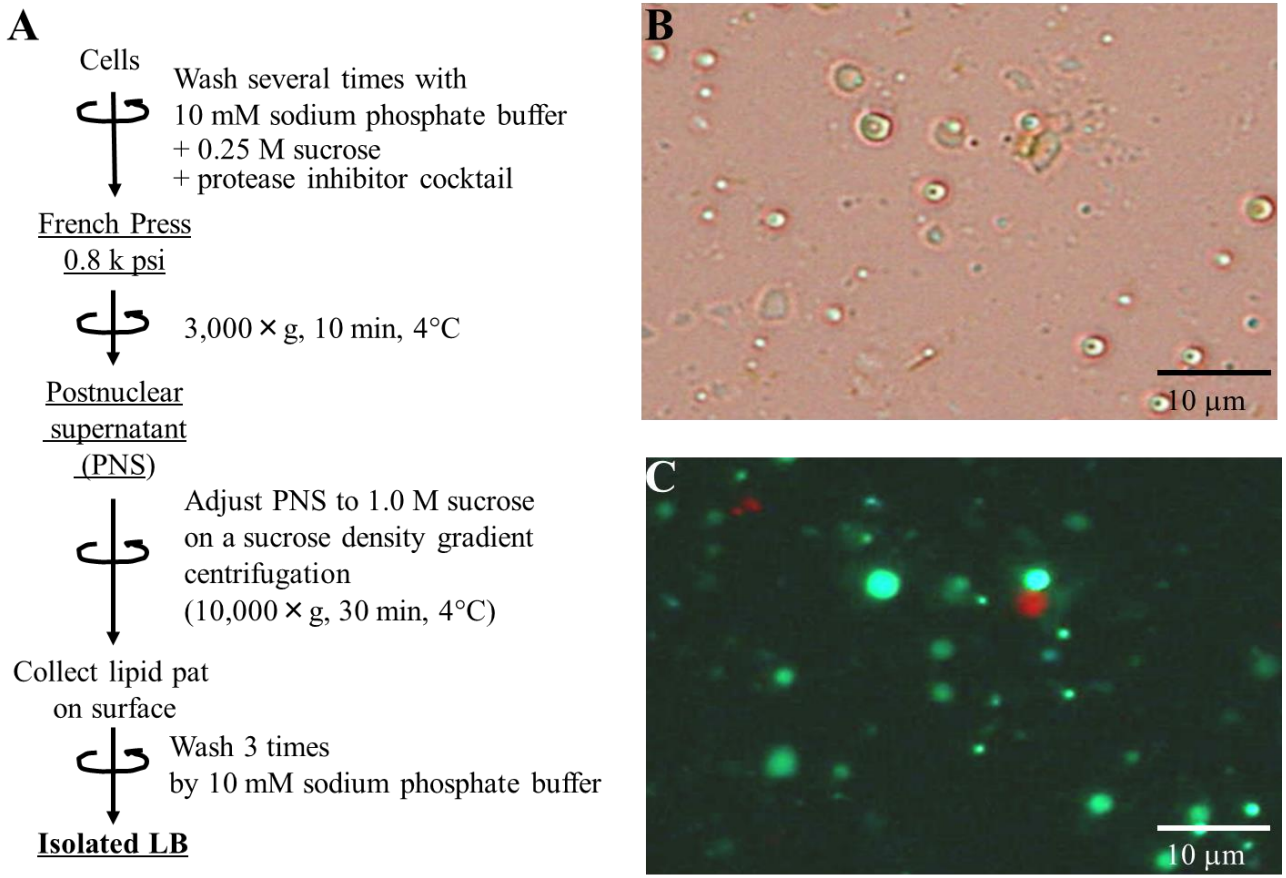

Figure 5. Newly established protocol for isolation of post-nuclear-supernatant (PNS) and ABs from N-deficient cells of haptophyte T. lutea. (A) Workflow of method for AB isolation. For sucrose gradient centrifugation, PNS in 1 M sucrose was placed in 1 M sucrose layer before centrifugation. (B) and (C): Bright view and fluorescent microscopic images of PNS stained with BODIPY 493/503. Green, ABs; red, chlorophyll auto-fluorescence.

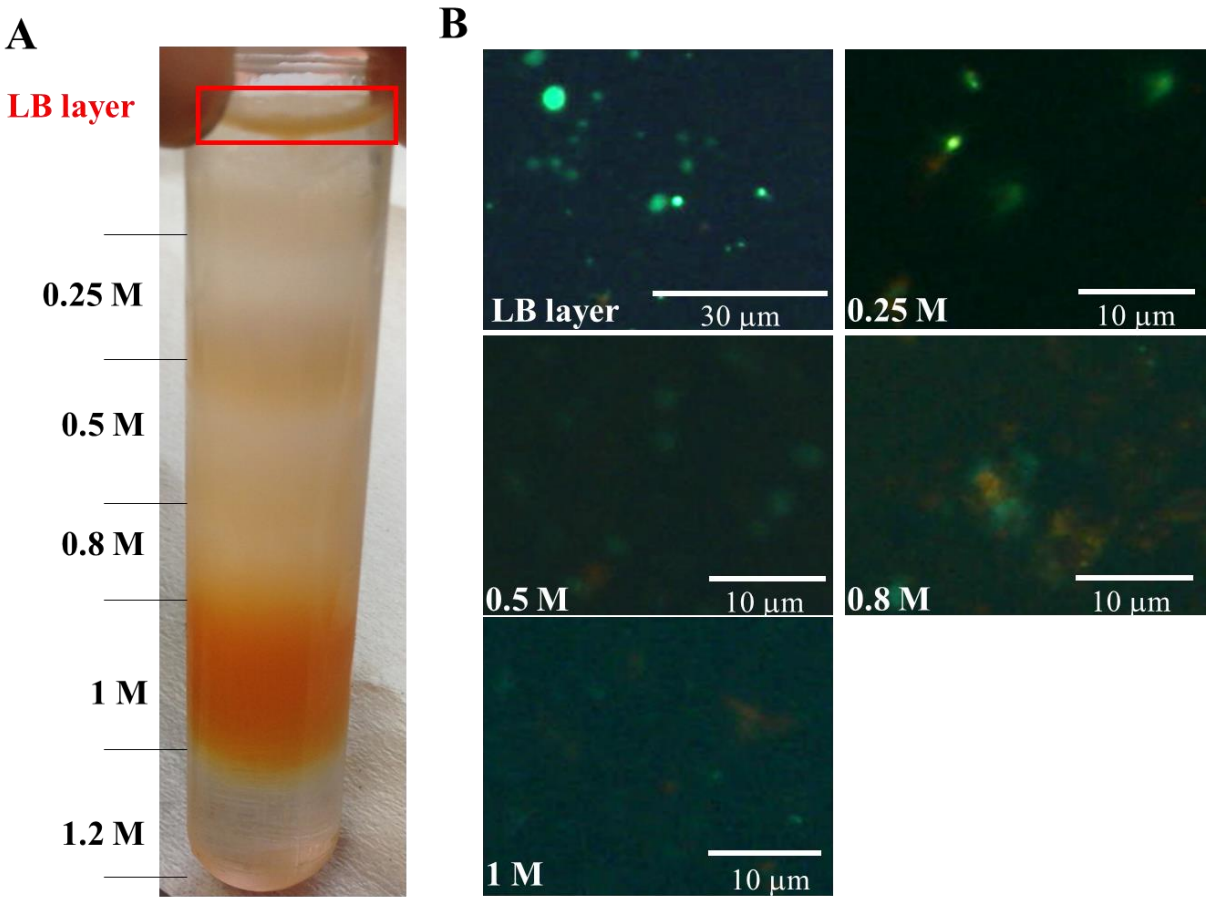

Figure 6. Purification of ABs by sucrose gradient centrifugation of PNS from N-deficient cells of haptophyte *T. lutea*. (A) Image of fractionation of ABs after stepwise sucrose density centrifugation. ABs were collected as a lipid pat on top. (B) Fluorescent microscopic images of granules stained with BODIPY 493/503. Green, ABs; red, chlorophyll auto-fluorescence.

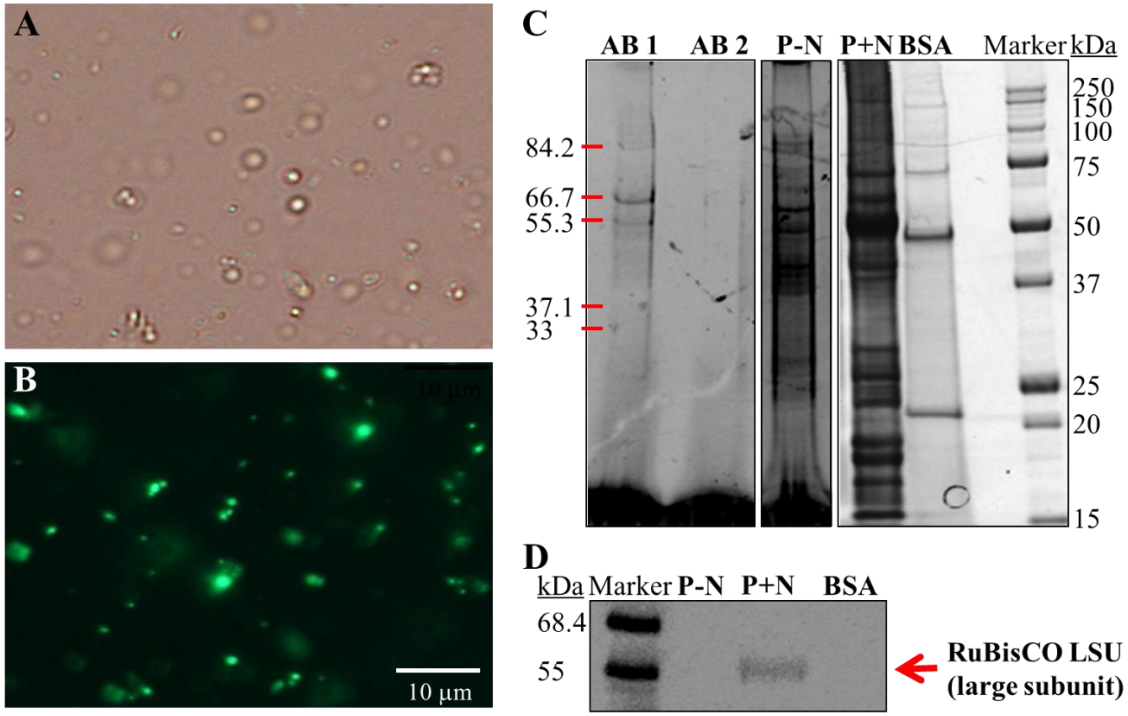

Figure 7. Microscopic images of purified ABs, profiles of proteins on SDS-PAGE and Western blot analysis of the purified ABs isolated from N-deficient cells of haptophyte *T. lutea*. (A) Bright view image. (B) Fluorescent microscopic image of ABs stained with BODIPY 493/503 showing no visible chlorophyll auto-fluorescence. (C) SDS-PAGE profile on 12.5% gel. Proteins applied: AB1 (3 µg), AB2 (2 µg), P-N (10 µg), P+N (10 µg) from T. lutea, and commercial BSA (10 µg) used as negative control. Marker: Molecular mass markers (with kDa). P-N and P+N: PNS from N-deficient cells (PNS/-N) and –sufficient cells (PNS/+N) as control, respectively. (D) Western blotting to reveal RuBisCO contamination or not in PNS/-N (P-N) and PNS/+N (P+N) from *T. lutea*, and BSA as control. Total proteins applied to each lane: 10 µg. Probe: antibody against RuBisCO large subunit.

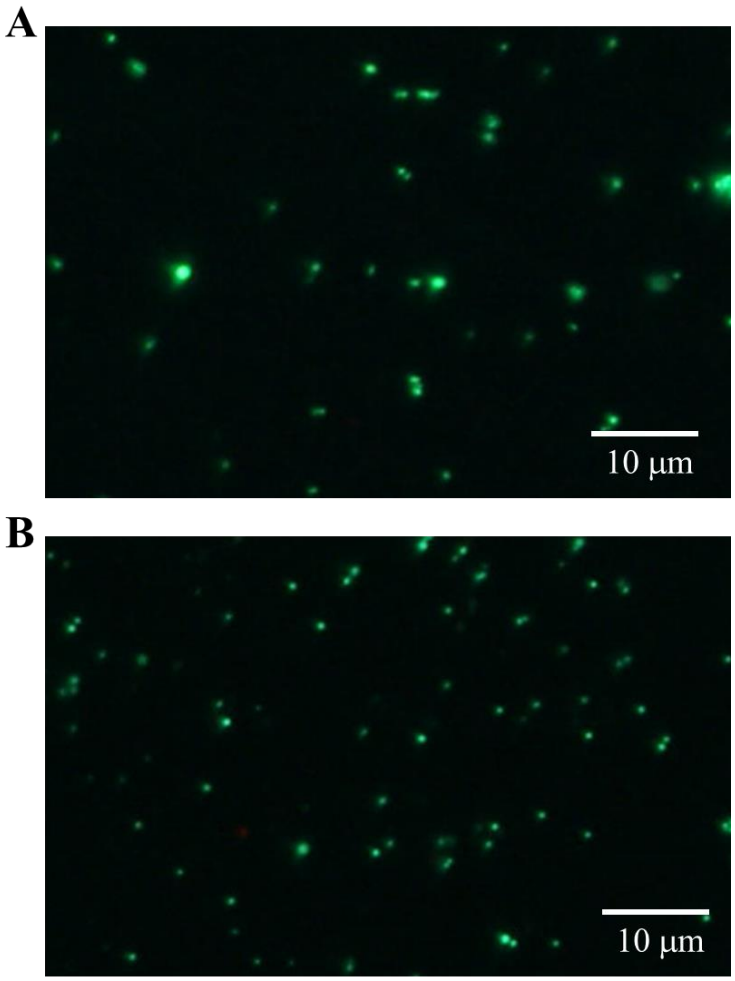

Figure 8. Purity confirmation of the ABs isolated by our newly developed method in two additional experiments. (A) and (B): Fluorescence microscopic images of ABs stained with BODIPY 493/503. No chlorophyll auto-fluorescence was observed under a fluorescent microscope in addition to no detection of chlorophylls by spectrophotometric determination.

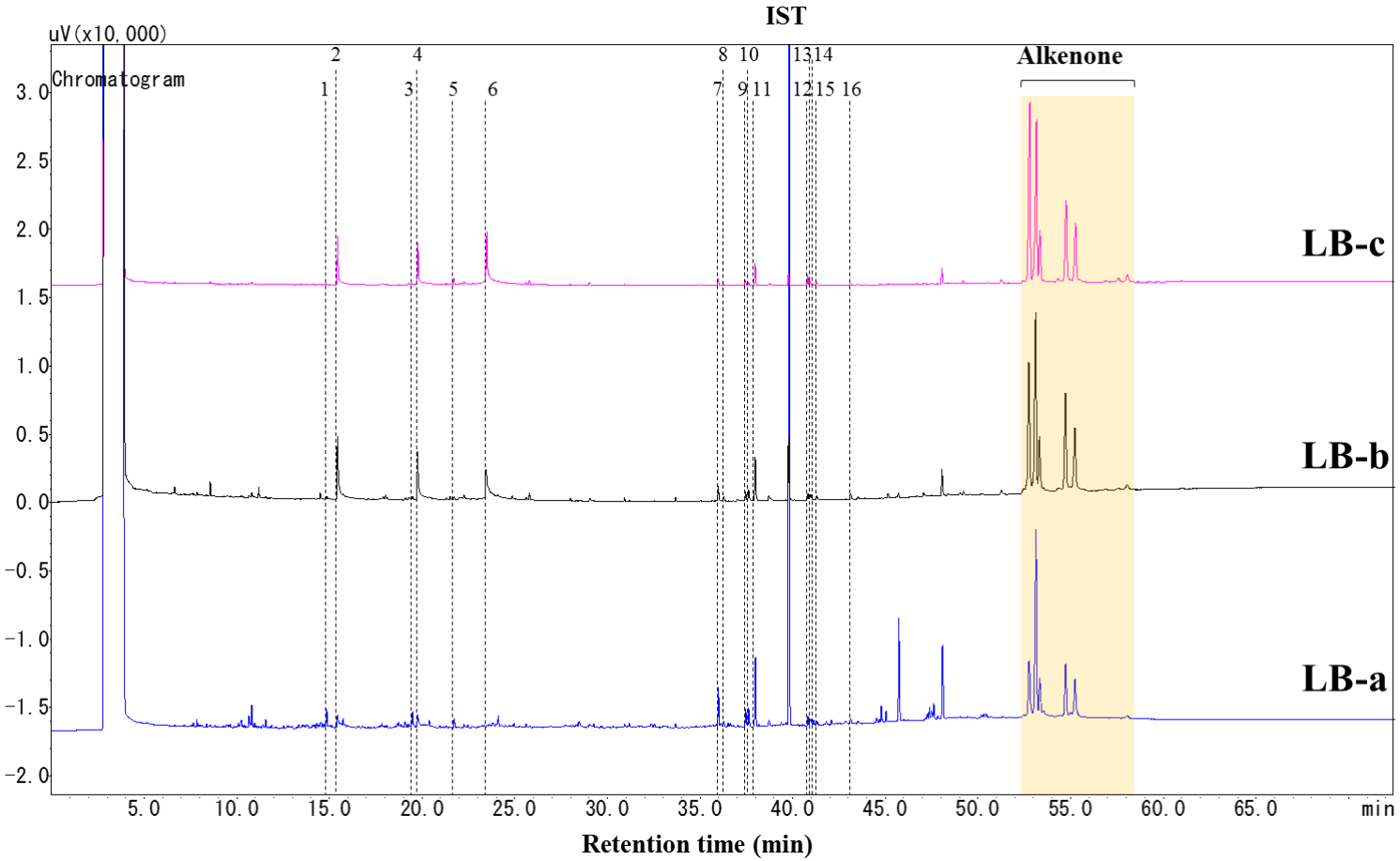

Figure 9. GC-chromatograms of lipids in purified LBs in independently prepared 3 samples (LB-a, -b, -c). Annotation of lipid species with peak numbers (1-16) is shown in Table 3.

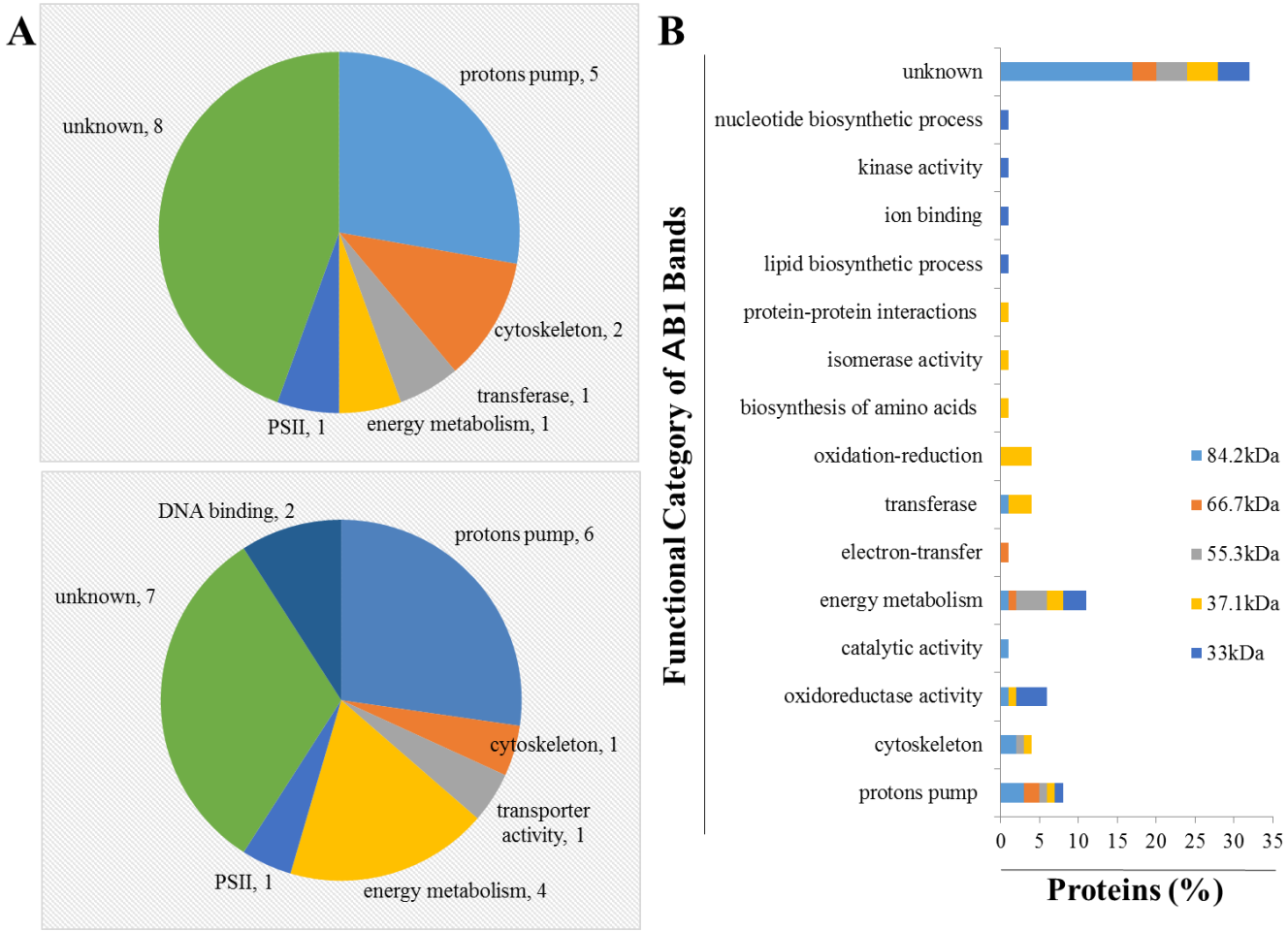

Figure 10. Category of hypothetical functions of abundant proteins in ABs from N-deficient cells of haptophyte . (A) AB1 and AB2. (B) Categories of hypothetical functions of proteins identified from the five abundant protein bands on SDS-PAGE of AB1.

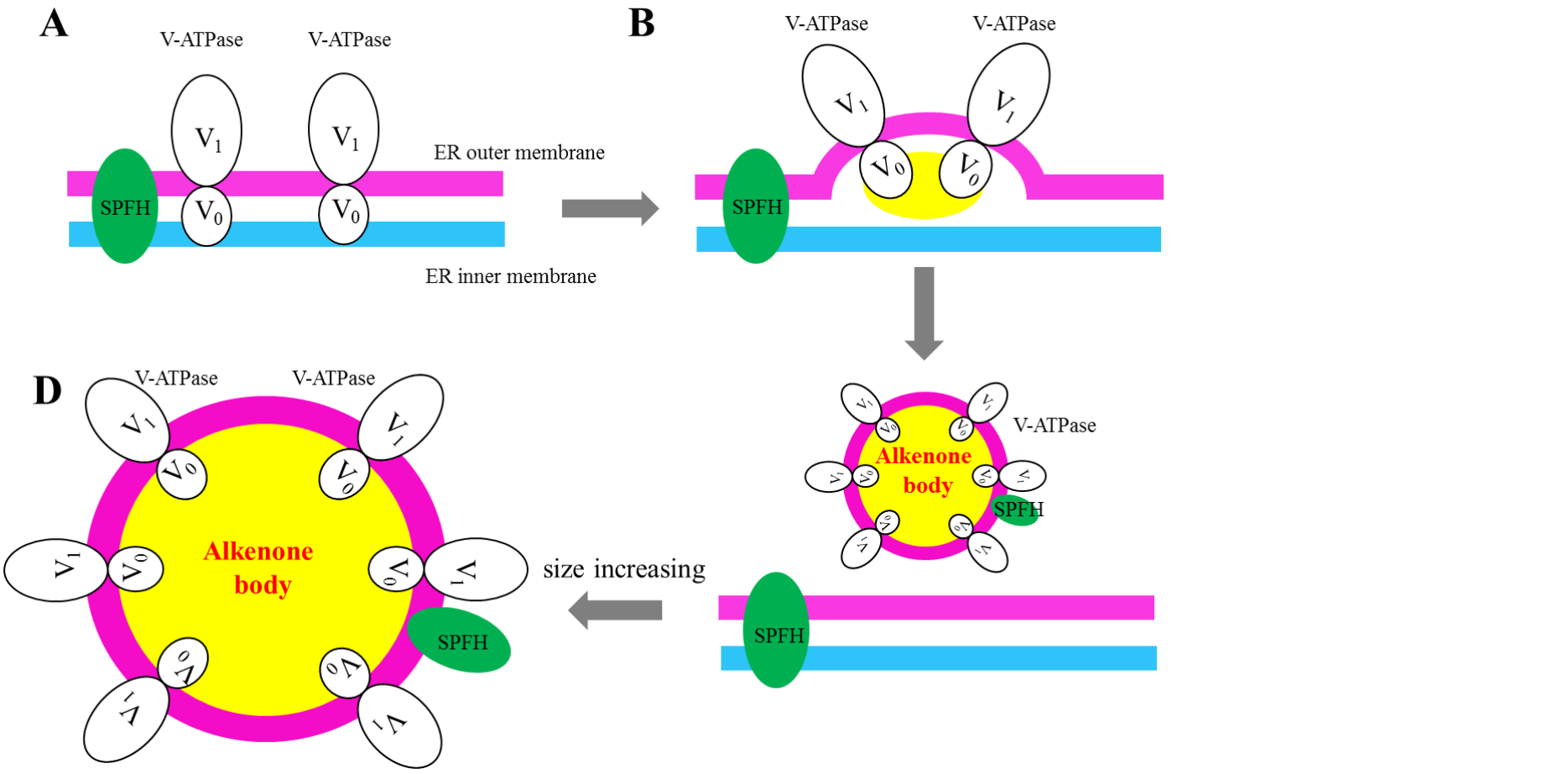

Figure 11. Hypothetical model of AB formation and development during N-deficient culture of haptophyte *T. lutea* according to fluorescence microscopic observation and proteomics. Symbols: V_0 and V_1, V_0 and V_1 subunits of V-ATPase, respectively. SPFH: SPFH domain-containing protein.

References

Agrawal GK, Bourguignon J, Rolland N, Ephritikhine G, Ferro M, Jaquinod M, Alexiou KG, Chardot T, Chakraborty N, Jolivet P, Doonan JH, Rakwal R (2011) Plant Organelle Proteomics: Collaborating for Optimal Cell Function. Mass Spectrometry Reviews **30:** 772-853

Alkhamis Y, Qin JG (2013) Cultivation of Isochrysis galbana in Phototrophic, Heterotrophic, and Mixotrophic Conditions. Biomed Research International

Amalraj RS, Selvaraj N, Veluswamy GK, Ramanujan RP, Muthurajan R, Palaniyandi M, Agrawal GK, Rakwal R, Viswanathan R (2010) Sugarcane proteomics: Establishment of a protein extraction method for 2-DE in stalk tissues and initiation of sugarcane proteome reference map. Electrophoresis **31:** 1959-1974

Baba M, Suzuki I, Shiraiwa Y (2011) Proteomic Analysis of High-CO_2-Inducible Extracellular Proteins in the Unicellular Green Alga, Chlamydomonas reinhardtii. Plant and Cell Physiology **52:** 1302-1314

Bauerle C, Ho MN, Lindorfer MA, Stevens TH (1993) The Saccharomyces-Cerevisiae Vma6 Gene Encodes the 36-Kda Subunit of the Vacuolar H^+-Atpase Membrane Sector. Journal of Biological Chemistry **268:** 12749-12757

Bell MV, Pond D (1996) Lipid composition during growth of motile and coccolith forms of Emiliania huxleyi. Phytochemistry **41:** 465-471

Bendif E, Probert I, Schroeder DC, de Vargas C (2013) On the description of Tisochrysis lutea gen. nov sp nov and Isochrysis nuda sp nov in the Isochrysidales, and the transfer of Dicrateria to the Prymnesiales (Haptophyta). Journal of Applied Phycology **25:** 1763-1776

Bougaran G, Rouxel C, Dubois N, Kaas R, Grouas S, Lukomska E, Le Coz JR, Cadoret JP (2012) Enhancement of neutral lipid productivity in the microalga *Isochrysis* affinis *Galbana* (T-Iso) by a mutation-selection procedure. Biotechnology and Bioengineering **109:** 2737-2745

Browman DT, Hoegg MB, Robbins SM (2007) The SPFH domain-containing proteins: more than lipid raft markers. Trends in Cell Biology **17:** 394-402

Browman DT, Resek ME, Zajchowski LD, Robbins SM (2006) Erlin-1 and erlin-2 are novel members of the prohibitin family of proteins that define lipid-raft-like domains of the ER. Journal of Cell Science **119:** 3149-3160

Brown MR, Dunstan GA, Jeffrey SW, Volkman JK, Barrett SM, Leroi JM (1993) The Influence of Irradiance on the Biochemical-Composition of the Prymnesiophyte *Isochrysis* Sp (Clone T-Iso). Journal of Phycology **29:** 601-612

Carrier G, Garnier M, Le Cunff L, Bougaran G, Probert I, De Vargas C, Corre E, Cadoret JP, Saint-Jean B (2014) Comparative Transcriptome of Wild Type and Selected Strains of the Microalgae *Tisochrysis lutea* Provides Insights into the Genetic Basis, Lipid Metabolism and the Life Cycle. Plos One **9**

Cermelli S, Guo Y, Gross SP, Welte MA (2006) The lipid-droplet proteome reveals that droplets are a protein-storage depot. Current Biology **16:** 1783-1795

Chapman KD, Dyer JM, Mullen RT (2012) Biogenesis and functions of lipid droplets in plants. Journal of Lipid Research **53:** 215-226

Conesa A, Götz S (2008) Blast2GO: A Comprehensive Suite for Functional Analysis in Plant Genomics. International Journal of Plant Genomics **2008:** 12

Corstjens PLAM, Gonzalez EL (2004) Effects of nitrogen and phosphorus availability on the expression of the coccolith-vesicle V-ATPase (subunit c) of Pleurochrysis (Haptophyta). Journal of Phycology **40:** 82-87

d'Andrea S, Canonge M, Beopoulos A, Jolivet P, Hartmann MA, Miquel M, Lepiniec L, Chardot T (2007) At5g50600 encodes a member of the short-chain dehydrogenase reductase superfamily with 11 beta- and 17 beta-hydroxy steroid dehydrogenase activities associated with Arabidopsis thaliana seed oil bodies. Biochimie **89:** 222-229

Danbara A, Shiraiwa Y (1999) The requirement of selenium for the growth of marine coccolithophorids, *Emiliania huxleyi*, *Gephyrocapsa oceanica* and *Helladosphaera* sp (Prymnesiophyceae). Plant and Cell Physiology **40:** 762-766

Davidi L, Katz A, Pick U (2012) Characterization of major lipid droplet proteins from *Dunaliella*. Planta **236:** 19-33

Ding YF, Zhang SY, Yang L, Na HM, Zhang P, Zhang HN, Wang Y, Chen Y, Yu JH, Huo CX, Xu SM, Garaiova M, Cong YS, Liu PS (2013) Isolating lipid droplets from multiple species. Nature Protocols **8:** 43-51

Dorrell RG, Smith AG (2011) Do Red and Green Make Brown?: Perspectives on Plastid Acquisitions within Chromalveolates. Eukaryotic Cell **10:** 856-868

Eltgroth ML, Watwood RL, Wolfe GV (2005) Production and cellular localization of neutral long-chain lipids in the haptophyte algae *Isochrysis galbana* and *Emiliania huxleyi.* Journal of Phycology **41:** 1000-1009

Epstein BL, D'Hondt S, Hargraves PE (2001) The possible metabolic role of C-37 alkenones in *Emiliania huxleyi*. Organic Geochemistry **32:** 867-875

Farese RV, Walther TC (2009) Lipid Droplets Finally Get a Little R-E-S-P-E-C-T. Cell **139:** 855-860

Fujiwara M, Uemura T, Ebine K, Nishimori Y, Ueda T, Nakano A, Sato MH, Fukao Y (2014) Interactomics of Qa-SNARE in *Arabidopsis thaliana.* Plant and Cell Physiology **55:** 781-789

Garnier M, Carrier G, Rogniaux H, Nicolau E, Bougaran G, Saint-Jean B, Cadoret JP (2014) Comparative proteomics reveals proteins impacted by nitrogen deprivation in wild-type and high lipid-accumulating mutant strains of *Tisochrysis lutea*. Journal of Proteomics **105:** 107-120

Gladu PK, Patterson GW, Wikfors GH, Chitwood DJ, Lusby WR (1990) The Occurrence of Brassicasterol and Epibrassicasterol in the Chromophycota. Comparative Biochemistry and Physiology B-Biochemistry & Molecular Biology **97:** 491-494

Goodman JM (2008) The gregarious lipid droplet. Journal of Biological Chemistry **283:** 28005-28009

Goodson C, Roth R, Wang ZT, Goodenough U (2011) Structural Correlates of Cytoplasmic and Chloroplast Lipid Body Synthesis in *Chlamydomonas reinhardtii* and Stimulation of Lipid Body Production with Acetate Boost.

Eukaryotic Cell **10:** 1592-1606

Gotz S, Garcia-Gomez JM, Terol J, Williams TD, Nagaraj SH, Nueda MJ, Robles M, Talon M, Dopazo J, Conesa A (2008) High-throughput functional annotation and data mining with the Blast2GO suite. Nucleic Acids Research **36:** 3420-3435

Haas BJ, Papanicolaou A, Yassour M, Grabherr M, Blood PD, Bowden J, Couger MB, Eccles D, Li B, Lieber M, MacManes MD, Ott M, Orvis J, Pochet N, Strozzi F, Weeks N, Westerman R, William T, Dewey CN, Henschel R, Leduc RD, Friedman N, Regev A (2013) De novo transcript sequence reconstruction from RNA-seq using the Trinity platform for reference generation and analysis. Nature Protocols **8:** 1494-1512

Heldt H-W, Piechulla B (2011) Plant biochemistry, Ed 4th. Elsevier Academic Press, The Netherlands

Holligan PM, Viollier M, Harbour DS, Camus P, Champagnephilippe M (1983) Satellite and Ship Studies of Coccolithophore Production Along a Continental-Shelf Edge. Nature **304:** 339-342

Horn PJ, James CN, Gidda SK, Kilaru A, Dyer JM, Mullen RT, Ohlrogge JB, Chapman KD (2013) Identification of a New Class of Lipid Droplet-Associated Proteins in Plants. Plant Physiology **162:** 1926-1936

Ishihama Y, Oda Y, Tabata T, Sato T, Nagasu T, Rappsilber J, Mann M (2005) Exponentially modified protein abundance index (emPAI) for estimation of absolute protein amount in proteomics by the number of sequenced peptides per protein. Molecular & Cellular Proteomics **4:** 1265-1272

Jolivet P, Acevedo F, Boulard C, d'Andrea S, Faure JD, Kohli A, Nesi N, Valot B, Chardot T (2013) Crop seed oil bodies: From challenges in protein identification to an emerging picture of the oil body proteome. Proteomics **13:** 1836-1849

Kane PM, Tarsio M, Liu JZ (1999) Early steps in assembly of the yeast vacuolar H^+-ATPase. Journal of Biological Chemistry **274:** 17275-17283

Katavic V, Agrawal GK, Hajduch M, Harris SL, Thelen JJ (2006) Protein and lipid composition analysis of oil bodies from two Brassica napus cultivars. Proteomics **6:** 4586-4598

Kotajima T, Shiraiwa Y, Suzuki I (2014) Functional screening of a novel Delta 15 fatty acid desaturase from the coccolithophorid Emiliania huxleyi. Biochimica Et Biophysica Acta-Molecular and Cell Biology of Lipids **1841:** 1451-1458

Krahmer N, Guo Y, Farese RV, Walther TC (2009) SnapShot: Lipid Droplets. Cell **139:** 1024-U1192

Langhorst MF, Reuter A, Stuermer CAO (2005) Scaffolding microdomains and beyond: the function of reggie/flotillin proteins. Cellular and Molecular Life Sciences **62:** 2228-2240

Lee SK, Li W, Ryu SE, Rhim T, Ahnn J (2010) Vacuolar (H^+)-ATPases in Caenorhabditis elegans: What can we learn about giant H+ pumps from tiny worms? Biochimica Et Biophysica Acta-Bioenergetics **1797:** 1687-1695

Li ZH, Thiel K, Thul PJ, Beller M, Kuhnlein RP, Welte MA (2012) Lipid Droplets

Control the Maternal Histone Supply of Drosophila Embryos. Current Biology **22:** 2104-2113

Lin IP, Jiang PL, Chen CS, Tzen JTC (2012) A unique caleosin serving as the major integral protein in oil bodies isolated from *Chlorella* sp cells cultured with limited nitrogen. Plant Physiology and Biochemistry **61:** 80-87

Lin LJ, Tai SSK, Peng CC, Tzen JTC (2002) Steroleosin, a sterol-binding dehydrogenase in seed oil bodies (vol 128, pg 1200, 2002). Plant Physiology **129:** 1930-1930

Liu CP, Lin LP (2001) Ultrastructural study and lipid formation of *Isochrysis* sp CCMP1324. Botanical Bulletin of Academia Sinica **42:** 207-214

Liu H, Probert I, Uitz J, Claustre H, Aris-Brosou S, Frada M, Not F, de Vargas C (2009) Extreme diversity in noncalcifying haptophytes explains a major pigment paradox in open oceans. Proceedings of the National Academy of Sciences of the United States of America **106:** 12803-12808

Marchetti J, Bougaran G, Le Dean L, Megrier C, Lukomska E, Kaas R, Olivo E, Baron R, Robert R, Cadoret JP (2012) Optimizing conditions for the continuous culture of Isochrysis affinis galbana relevant to commercial hatcheries. Aquaculture **326:** 106-115

Marlowe IT, Brassell SC, Eglinton G, Green JC (1984) Long chain unsaturated ketones and esters in living algae and marine sediments. Organic Geochemistry **6:** 135-141

Marlowe IT, Green JC, Neal AC, Brassell SC, Eglinton G, Course PA (1984) Long-Chain (N-C_{37}-C_{39}) Alkenones in the Prymnesiophyceae - Distribution of Alkenones and Other Lipids and Their Taxonomic Significance. British Phycological Journal **19:** 203-216

Marshansky V, Futai M (2008) The V-type H^+-ATPase in vesicular trafficking: targeting, regulation and function. Current Opinion in Cell Biology **20:** 415-426

Metzger P, Largeau C (2005) Botryococcus braunii: a rich source for hydrocarbons and related ether lipids. Applied Microbiology and Biotechnology **66:** 486-496

Moellering ER, Benning C (2010) RNA Interference Silencing of a Major Lipid Droplet Protein Affects Lipid Droplet Size in Chlamydomonas reinhardtii. Eukaryotic Cell **9:** 97-106

Morrow IC, Parton RG (2005) Flotillins and the PHB domain protein family: Rafts, worms and anaesthetics. Traffic **6:** 725-740

Murphy S, Martin S, Parton RG (2009) Lipid droplet-organelle interactions; sharing the fats. Biochimica Et Biophysica Acta-Molecular and Cell Biology of Lipids **1791:** 441-447

Naested H, Frandsen GI, Jauh GY, Hernandez-Pinzon I, Nielsen HB, Murphy DJ, Rogers JC, Mundy J (2000) Caleosins: Ca^{2+}-binding proteins associated with lipid bodies. Plant Molecular Biology **44:** 463-476

Nguyen HM, Baudet M, Cuine S, Adriano JM, Barthe D, Billon E, Bruley C, Beisson F, Peltier G, Ferro M, Li-Beisson Y (2011) Proteomic profiling of oil bodies isolated from the unicellular green microalga *Chlamydomonas reinhardtii:* With focus on proteins involved in lipid metabolism. Proteomics **11:**

4266-4273

Nojima D, Yoshino T, Maeda Y, Tanaka M, Nemoto M, Tanaka T (2013) Proteomics Analysis of Oil Body-Associated Proteins in the Oleaginous Diatom. Journal of Proteome Research **12:** 5293-5301

Not F, Siano R, Kooistra WHCF, Simon N, Vaulot D, Probert I (2012) Diversity and Ecology of Eukaryotic Marine Phytoplankton. Genomic Insights into the Biology of Algae **64:** 1-53

O'Neil GW, Knothe G, Williams JR, Burlow NP, Culler AR, Corliss JM, Carmichael CA, Reddy CM (2014) Synthesis and Analysis of an Alkenone-Free Biodiesel from Isochrysis sp. Energy & Fuels **28:** 2677-2683

Pasaribu B, Lin IP, Tzen JC, Jauh G-Y, Fan T-Y, Ju Y-M, Cheng J-O, Chen C-S, Jiang P-L (2014) SLDP: a Novel Protein Related to Caleosin Is Associated with the Endosymbiotic Symbiodinium Lipid Droplets from Euphyllia glabrescens. Marine Biotechnology **16:** 560-571

Peled E, Leu S, Zarka A, Weiss M, Pick U, Khozin-Goldberg I, Boussiba S (2011) Isolation of a Novel Oil Globule Protein from the Green Alga *Haematococcus pluvialis* (Chlorophyceae). Lipids **46:** 851-861

Peng SE, Chen WNU, Chen HK, Lu CY, Mayfield AB, Fang LS, Chen CS (2011) Lipid bodies in coral-dinoflagellate endosymbiosis: Proteomic and ultrastructural studies. Proteomics **11:** 3540-3555

Peters C, Bayer MJ, Buhler S, Andersen JS, Mann M, Mayer A (2001) Trans-complex formation by proteolipid channels in the terminal phase of membrane fusion. Nature **409:** 581-588

Prahl F, Herbert T, Brassell SC, Ohkouchi N, Pagani M, Repeta D, Rosell-Mele A, Sikes E (2000) Status of alkenone paleothermometer calibration: Report from Working Group 3. Geochemistry Geophysics Geosystems **1**

Prahl FG, Wakeham SG (1987) Calibration of Unsaturation Patterns in Long-Chain Ketone Compositions for Paleotemperature Assessment. Nature **330:** 367-369

Pribyl P, Cepak V, Zachleder V (2013) Production of lipids and formation and mobilization of lipid bodies in Chlorella vulgaris. Journal of Applied Phycology **25:** 545-553

Rechka JA, Maxwell JR (1988) Characterization of Alkenone Temperature Indicators in Sediments and Organisms. Organic Geochemistry **13:** 727-734

Rodolfi L, Zittelli GC, Bassi N, Padovani G, Biondi N, Bonini G, Tredici MR (2009) Microalgae for Oil: Strain Selection, Induction of Lipid Synthesis and Outdoor Mass Cultivation in a Low-Cost Photobioreactor. Biotechnology and Bioengineering **102:** 100-112

Sawada K, Shiraiwa Y (2004) Alkenone and alkenoic acid compositions of the membrane fractions of *Emiliania huxleyi*. Phytochemistry **65:** 1299-1307

Shimada TL, Takano Y, Shimada T, Fujiwara M, Fukao Y, Mori M, Okazaki Y, Saito K, Sasaki R, Aoki K, Hara-Nishimura I (2014) Leaf Oil Body Functions as a Subcellular Factory for the Production of a Phytoalexin in Arabidopsis. Plant Physiology **164:** 105-118

Siloto RMP, Findlay K, Lopez-Villalobos A, Yeung EC, Nykiforuk CL, Moloney

MM (2006) The accumulation of oleosins determines the size of seed oilbodies in *Arabidopsis*. Plant Cell **18:** 1961-1974

Song PP, Li L, Liu JG (2013) Proteomic Analysis in Nitrogen-Deprived Isochrysis galbana during Lipid Accumulation. Plos One **8**

Song ZH, Nes WD (2007) Inactivation of soybean sterol 24-C-methyltransferase by elongated sterol side chains at C26. Bioorganic & Medicinal Chemistry Letters **17:** 5902-5906

Sukenik A, Wahnon R (1991) Biochemical quality of marine unicellular algae with special emphasis on lipid composition. I. Isochrysis galbana. Aquaculture **97:** 61-72

Theroux S, D'Andrea WJ, Toney J, Amaral-Zettler L, Huang YS (2010) Phylogenetic diversity and evolutionary relatedness of alkenone-producing haptophyte algae in lakes: Implications for continental paleotemperature reconstructions. Earth and Planetary Science Letters **300:** 311-320

Tsuji Y, Suzuki I, Shiraiwa Y (2012) Enzymological Evidence for the Function of a Plastid-Located Pyruvate Carboxylase in the Haptophyte alga *Emiliania huxleyi*: A Novel Pathway for the Production of C-4 Compounds. Plant and Cell Physiology **53:** 1043-1052

Valenzuela J, Mazurie A, Carlson RP, Gerlach R, Cooksey KE, Peyton BM, Fields MW (2012) Potential role of multiple carbon fixation pathways during lipid accumulation in Phaeodactylum tricornutum. Biotechnology for Biofuels **5**

Vieler A, Brubaker SB, Vick B, Benning C (2012) A Lipid Droplet Protein of Nannochloropsis with Functions Partially Analogous to Plant Oleosins. Plant Physiology **158:** 1562-1569

Viotti C, Kruger F, Krebs M, Neubert C, Fink F, Lupanga U, Scheuring D, Boutte Y, Frescatada-Rosa M, Wolfenstetter S, Sauer N, Hillmer S, Grebe M, Schumacher K (2013) The Endoplasmic Reticulum Is the Main Membrane Source for Biogenesis of the Lytic Vacuole in Arabidopsis. Plant Cell **25:** 3434-3449

Wang ZT, Ullrich N, Joo S, Waffenschmidt S, Goodenough U (2009) Algal Lipid Bodies: Stress Induction, Purification, and Biochemical Characterization in Wild-Type and Starchless *Chlamydomonas reinhardtii*. Eukaryotic Cell **8:** 1856-1868

Wojciech.Za, Goad LJ, Goodwin TW (1973) S-Adenosyl-L-Methionine-Cycloartenol Methyltransferase Activity in Cell-Free Systems from *Trebouxia* Sp and Scenedesmus-Obliquus. Biochemical Journal **136:** 405-412

Zechner R, Zimmermann R, Eichmann TO, Kohlwein SD, Haemmerle G, Lass A, Madeo F (2012) FAT SIGNALS - Lipases and Lipolysis in Lipid Metabolism and Signaling. Cell Metabolism **15:** 279-291

Zehmer JK, Huang YG, Peng G, Pu J, Anderson RGW, Liu PS (2009) A role for lipid droplets in inter-membrane lipid traffic. Proteomics **9:** 914-921

Acknowledgement

I would like to express my deep gratitude to Professor Dr. Yoshihiro Shiraiwa, University of Tsukuba, for his great guidance and continuous encouragement throughout all my study and research work. I also want to thank Professor Dr. Iwane Suzuki, University of Tsukuba, for all his valuable advices and kindly encouragement.

I want to give my thanks to associate professor Dr. Hiroya Araie, University of Tsukuba, for all his enlightening suggestions, kindly help and discussions.

I sincerely appreciate Professor Dr. Randeep Rakwal, University of Tsukuba, for all his kindness, encouragement and valuable suggestions.

I want to thank Dr. Yichiro Fukao, Ritsumeikan University, who carried out LC-MSMS experiment, for all his help and valuable suggestions.

I also thank all members of the Laboratory of Plant Physiology and Metabolism of University of Tsukuba, for all three years accompany, kindly supports and many sided helps.

Best thanks must be given to my parents, for all their support, encouragement, especially their caring listening. I would like to thank my brothers and sisters, for all their pray for me laid before Lord.

Last but not the least, praise the Lord. In the beginning God created the heavens and the earth. I like what I studied in these years and all species the Lord created are unique and charming, like what he said in Genesis, “And God saw everything that he had made, and, behold, it was very good.” Three years oversea Ph.D study is not an easy job, for thousands of times I wanted to quit, but still with the help of my King, I finally made it. I saw the glory of Lord with my own eyes, and experienced his all mighty, in every impossible moment he turned it to possible. Blessed is the man that trust in the Lord, and whose hope the Lord is.